ACS OMEGA

http://pubs.acs.org/journal/acsodf

Article

Ancillary-Ligand-Assisted Variation in Nuclearities Leading to the Formation of Di-, Tri-, and Tetranuclear Copper(II) Complexes with Multifaceted Carboxylate Coordination Chemistry

Avishek Majumder, Sujan Sk, Arpan Das, Gonela Vijaykumar, Malaya K. Sahoo, J. N. Behera, and Manindranath Bera*

Cite This: *ACS Omega* 2022, 7, 39985−39997

Read Online

ACCESS | Metrics & More | Article Recommendations | Supporting Information

ABSTRACT: The self-assembly of a carboxylate-based dinucleating ligand, *N*,*N*′-bis[2-carboxybenzomethyl]-*N*,*N*′-bis[2-pyridylmethyl]-1,3-diaminopropan-2-ol (H_3cpdp), and copper(II) ions in the presence of various exogenous ancillary ligands results in the formation of the new dinuclear complex $[Cu_2(cpdp)(\mu\text{-Hisophth})]_4\cdot 2H_2$isophth$\cdot 21H_2O$ (**1**), trinuclear complex $[Cu_3(Hcpdp)(Cl)_4]$ (**2**), and tetranuclear complex $[Cu_4(cpdp)(\mu\text{-Hphth})(\mu_4\text{-phth})(piconol)(Cl)_2]\cdot 3H_2O$ (**3**) (H_2phth = phthalic acid; H_2isophth = isophthalic acid; piconol = 2-pyridinemethanol; Cl^- = chloride). In methanol−water, the reaction of H_3cpdp with $CuCl_2\cdot 2H_2O$ at room temperature leads to the formation of **2**. On the other hand, **1** and **3** have been obtained by carrying out the reaction of H_3cpdp with $CuCl_2\cdot 2H_2O$/*m*-$C_6H_4(CO_2Na)_2$ and $CuCl_2\cdot 2H_2O$/*o*-$C_6H_4(CO_2Na)_2$/piconol, respectively, in methanol−water in the presence of NaOH at ambient temperature. All three complexes have been characterized by elemental analysis, molar electrical conductivity and magnetic moment measurements, FTIR, UV−vis spectroscopy, and PXRD, including single-crystal X-ray structural analyses. The molecular structure of **1** is based on a μ-alkoxide and μ-isophthalate-bridged dimeric $[Cu_2]$ core; the structure of **2** represents a trimeric $[Cu_3]$ core in which a μ-alcohol-bridged dinuclear $[Cu_2]$ unit is exclusively coupled with a $[CuCl_2]$ species by two $\mu{:}\eta^1{:}\eta^1$-*syn-anti* carboxylate groups forming a triangular motif; the structure of **3** embodies a tetrameric $[Cu_4]$ core, with two copper(II) ions in a distorted-octahedral coordination environment, one copper(II) ion in a distorted-trigonal-bipyramidal coordination environment, and the other copper(II) ion in a square-planar coordination environment. In fact, **2** and **3** represent rare examples of copper(II)-based multinuclear complexes showing outstanding features of rich coordination chemistry: (i) using a symmetrical dinucleating ligand, trinuclear complex **2** is generated with four- and five-coordination environments around copper(II) ions; (ii) the unsymmetrical tetranuclear complex **3** is obtained by using the same ligand with four-, five- and six-coordination environments around copper(II) ions; (iii) tetracopper(II) complex **3** shows four different bridging modes of carboxylate groups simultaneously such as $\mu{:}\eta^2$, $\mu{:}\eta^1{:}\eta^1$, $\mu_3{:}\eta^2{:}\eta^1{:}\eta^1$, and $\mu_4{:}\eta^1{:}\eta^1{:}\eta^1{:}\eta^1$, the $\mu_4{:}\eta^1{:}\eta^1{:}\eta^1{:}\eta^1$ mode of phthalate being unprecedented. The formation of these $[Cu_2]$, $[Cu_3]$, and $[Cu_4]$ complexes can be controlled by changing the exogenous ancillary ligands and pH of the reaction solutions, thus allowing an effective tuning of the self-assembly. The magnetic susceptibility measurements suggest that the copper centers in all three complexes are antiferromagnetically coupled. The thermal properties of **1**−**3** have been investigated by thermogravimetric and differential thermal analytical (TGA and DTA) techniques, indicating that the decomposition of all three complexes proceeds via multistep processes.

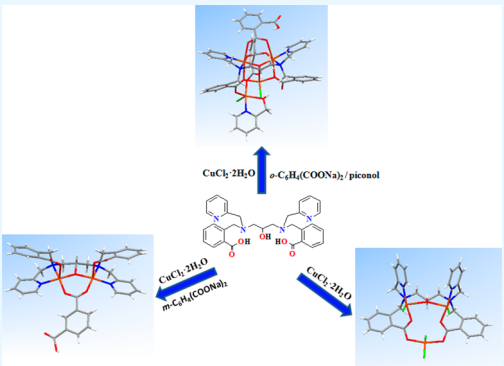

INTRODUCTION

Metal-assisted self-assembly processes constitute successful approaches to the preparation of well-defined coordination complexes having aesthetically attractive architectures from both material and biological origins.[1−10] Such metal−ligand coordination-driven self-assembly is one of the most compelling synthetic tools, among other self-assembly processes, that are used for the production of a plethora of discrete molecular topologies.[11−15] Among the different transition metals, copper is a good candidate for the assembly of multinuclear complexes due to its varied coordination number, which can be conjugated with flexibility of the ligand systems. Usually, the coordination chemistry of copper is dominated by the Cu(II) ion forming a rich variety of its

Received: July 22, 2022
Accepted: October 17, 2022
Published: October 28, 2022

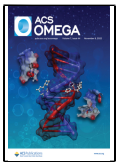

https://doi.org/10.1021/acsomega.2c04627
ACS Omega 2022, 7, 39985−39997

coordination complexes. As the copper(II) complexes are often labile and unusual in their preference for distorted coordination geometries, they are much less structurally predictable than other 3d transition-metal complexes. The multinuclear complexes of Cu(II) display fascinating electronic and magnetic properties.[16−18] In addition to molecular magnetism,[19−21] multinuclear copper(II) complexes have also proved to be of substantial interest in several modern research areas such as catalysis,[22] DNA cleavage,[23] oxygen activation,[24] and host−guest equilibria.[25] The choice of different polyfunctional ligands containing oxygen and nitrogen donor atoms allows a rational approach to obtain definite and interesting molecular structural designs.[26−28] Consequently, a great deal of attention has been paid to the preparation and systematic characterization of multinuclear copper(II) complexes.[29−31]

Carboxylate-containing ligands have been investigated for some time as a way to assemble different 3d metal ions into aggregates with relevance in the area of coordination chemistry, because their flexibility and conformational freedom support the formation of diverse multinuclear complex architectures with novel topologies.[32−40] In principle, molecular-level control over the formation of three-dimensional structures should provide a rational design and synthesis of a wide variety of these multinuclear complexes with modified properties. Carboxylate-based copper(II) complexes may be mono-, di-, or multinuclear because of their wide-ranging coordination modes. In comparison to mononuclear complexes, the duly designed di- and multinuclear complexes not only present synthetic challenges but also can put forward new reactivity patterns. For example, dinuclear triply bridged copper(II) complexes can exhibit a great diversity of topologies, in which the coordination around the metal centers continuously changes from regular trigonal bipyramidal to square pyramidal.[41] Hence, from a synthetic and structural point of view, although dinuclear copper(II) chemistry is a quite extensively studied research field,[42] reports on trinuclear and higher-nuclearity copper(II) complexes are relatively limited.[43,44]

The focus here is on the symmetrical dinucleating ligand *N*,*N*′-bis[2-carboxybenzomethyl]-*N*,*N*′-bis[2-pyridylmethyl]-1,3-diaminopropan-2-ol (H_3cpdp), incorporating two pyridine and two benzoate functionalities (Scheme 1).[45] Recently, we

Scheme 1. Chemical Structures with Observed Anionic Forms of the Ligand H_3cpdp

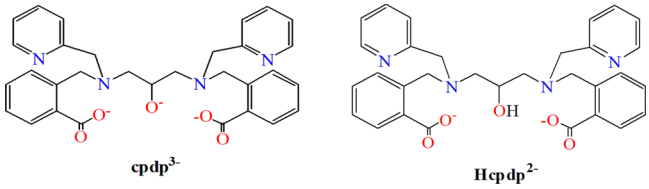

have shown that the ligand H_3cpdp coordinates with Co(II), Fe(III), Cu(II), and Zn(II), including Li/Na, forming a variety of higher-nuclearity complexes with smart molecular structures and interesting material/biological properties.[27b,33,34,46−48] In those complexes, the ligand H_3cpdp has either a trianionic ($cpdp^{3-}$) or a dianionic ($Hcpdp^{2-}$) form (Scheme 1), exhibiting flexible coordination modes of the carboxylate groups. While further exploring the reactions of H_3cpdp with copper(II) ions in the presence of different exogenous ancillary ligands such as isophthalate, chloride, and phthalate/chloride/piconol, we isolated new di-, tri-, and tetranuclear copper(II) complexes of the formulas $[Cu_2(cpdp)(\mu\text{-Hisophth})]_4\cdot 2H_2$isophth$\cdot 21H_2O$ (**1**), $[Cu_3(Hcpdp)(Cl)_4]$ (**2**), and $[Cu_4(cpdp)(\mu\text{-Hphth})(\mu_4\text{-phth})(piconol)(Cl)_2]\cdot 3H_2O$ (**3**). Different ancillary ligands have been employed for the construction of these complexes because, initially, the ligand $cpdp^{3-}$ or $Hcpdp^{2-}$ coordinates two copper(II) ions, leaving behind accessible binding sites for additional coordination of isophthalate, chloride, or phthalate/chloride/piconol offering subsequent aggregation processes for the self-assembly. Thus, the utilization of the carboxylate-based ligand H_3cpdp in combination with isophthalate, chloride, or phthalate/chloride/piconol not only assists in the formation of the complexes but also supports the necessary factors for their stabilization. In connection to coordination with copper(II), the different binding modes of carboxylate groups of the $Hcpdp^{2-}/cpdp^{3-}$ and phthalate/isophthalate observed in **1**−**3** are shown in Scheme 2 (modes **A** and **F** in complex **1**; mode **B** in complex **2**; modes **C**−**E** in complex **3**). Therefore, this article describes a simple and facile approach to synthesize a new series of di-, tri-, and tetranuclear copper(II) complexes of a symmetrical carboxylate-based dinucleating ligand showing interesting and outstanding coordination chemistry. Furthermore, their in-depth structural aspects and spectroscopic and thermal properties are described.

RESULTS AND DISCUSSION

General Synthesis of the Ligand and Complexes. The carboxylate-based symmetrical dinucleating ligand H_3cpdp was prepared following our previously published procedure.[45] Characterization of the ligand was accomplished by elemental analysis, FTIR, NMR, ESI-MS, and thermogravimetric techniques. The FTIR, ^{1}H and ^{13}C NMR, ESI-MS, and thermogravimetric data are provided in Figures S1−S5 of the Supporting Information. The reactions of H_3cpdp with copper(II) salts have been systematically investigated, as summarized in Scheme 3. When the reaction of H_3cpdp with $CuCl_2\cdot 2H_2O$ was carried out in CH_3OH/H_2O (9/1; v/v) in the absence of any base, complex **2** was obtained (Scheme 3). Several H_3cpdp/Cu ratios were explored, and here we report only the optimized ratios that a yielded clean and well-characterized product in high yield. At room temperature, **2** was easily isolated as a green compound by stirring a CH_3OH/H_2O solution of H_3cpdp and $CuCl_2\cdot 2H_2O$ in a 1/3 molar ratio for 1 h at pH ∼3. This synthetic procedure was further explored with *m*-$C_6H_4(CO_2Na)_2$ and *o*-$C_6H_4(CO_2Na)_2$/piconol successively in the presence of NaOH. In CH_3OH/H_2O (9/1; v/v), bluish green complexes **1** and **3** (Scheme 3) were obtained in good yield by room-temperature stirring of reaction solutions of H_3cpdp, $CuCl_2\cdot 2H_2O$, and *m*-$C_6H_4(CO_2Na)_2$ or *o*-$C_6H_4(CO_2Na)_2$/piconol, in 1/2/1 or 1/4/2/1 molar ratios, respectively, for 1 h in the presence of NaOH at pH ∼6.5, under aerobic conditions. The nature of the final products for all three complexes is strongly influenced by the presence of exogenous coligands such as phthalate, isophthalate, piconol, and chloride, in either bridging and nonbridging modes, and the pH of the reaction solution, resulting in the formation of di-, tri-, and tetranuclear cores. Therefore, the formation of these three copper(II) complexes can be directly controlled by choosing the appropriate ancillary ligands and maintaining the experimental pH. Complexes **1**−**3** were fully characterized by elemental analysis, solution electrical conductivity, FTIR, and UV−vis, together with

https://doi.org/10.1021/acsomega.2c04627
ACS Omega 2022, 7, 39985−39997

Scheme 2. Different Binding Modes of Carboxylate Groups of $Hcpdp^{2-}$/$cpdp^{3-}$ (A−C), Phthalate (D, E), and Isophthalate (F) Observed in Complexes 1−3

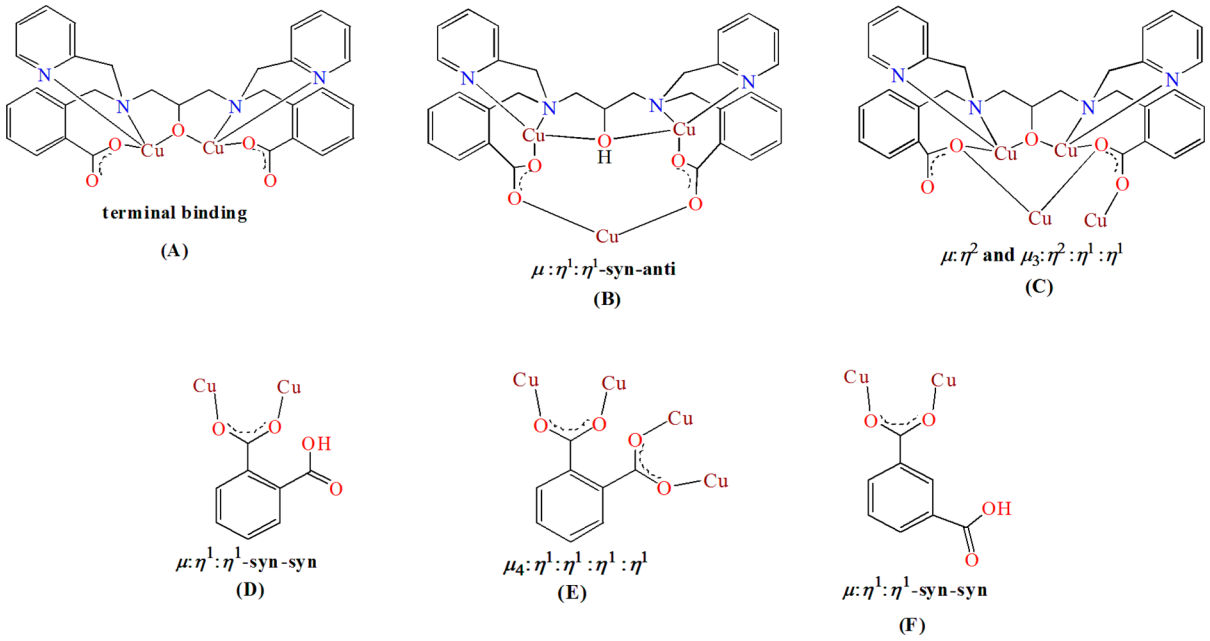

powder and single-crystal X-ray crystallography. The elemental analysis, solution molar electrical conductivity, and single-crystal X-ray diffraction studies confirm their compositions. At room temperature, the molar conductivity values of **1−3** in MeOH are in the range of 15−22 Ω^{-1} cm^2 mol^{-1}, indicating the nonelectrolytic formulations of the complexes.[49]

FTIR Spectroscopy. The FTIR spectra of **1−3** show broad absorption bands in the range of 3401−3434 cm^{-1}, indicating the O−H stretching vibrations of lattice waters/alcohol groups.[50] The spectra of **1** show two asymmetric $\nu_{as}(COO^-)$ and two symmetric $\nu_s(COO^-)$ stretching vibrations at 1609 and 1553 cm^{-1} and at 1447 and 1377 cm^{-1}, respectively. The differences between $\nu_{as}(COO^-)$ and $\nu_s(COO^-)$ stretches (Δ) of ∼232 and ∼106 cm^{-1} for **1** suggest two different coordination modes: monodentate terminal coordination of benzoate and μ:η^1:η^1-*syn-syn* bidentate coordination of isophthalate groups, respectively.[51−53] The band observed at a higher wave number of 1609 cm^{-1}, which can be assigned to the ν(C═N) stretching vibration of the pyridine moiety of the ligand backbone, is most probably overlapped with the ν(C═O) stretching vibration of one −COOH group of the isophthalate moiety. For **2**, typical absorptions at 1559 and 1450 cm^{-1} in the FTIR spectrum can be associated with $\nu_{as}(COO^-)$ and $\nu_s(COO^-)$ vibrations of the coordinated benzoates, respectively. The Δ value of ∼109 cm^{-1} is in agreement with the μ:η^1:η^1-*syn-anti* bidentate function of the benzoate group.[51−53] The spectrum of **2** also exhibits a characteristic band at 1612 cm^{-1}, attributed to the ν(C═N) stretching vibration of the pyridine moiety of the ligand backbone. On the other hand, the different coordination modes of benzoate and phthalate functionalities, namely, monodentate μ:η^2, bidentate μ:η^1:η^1, tridentate μ_3:η^2:η^1:η^1, and tetradentate μ_4:η^1:η^1:η^1:η^1 bridging coordinations, have been recognized in the FTIR spectrum of **3**. The FTIR spectrum of **3** shows two intense asymmetric $\nu_{as}(COO^-)$ bands at 1615 and 1564 cm^{-1} and two intense symmetric $\nu_s(COO^-)$ bands at 1452 and 1367 cm^{-1}. The higher wavenumber band at 1615 cm^{-1} is also overlapped with the ν(C═N) stretching vibration of the pyridine moiety of the ligand backbone/piconol and the ν(C═O) stretching vibration of one −COOH group of the phthalate moiety. Whereas the significantly higher difference Δ of ∼248 cm^{-1} is attributed to the monodentate μ:η^2 bridging coordination of benzoate, the relatively lower difference Δ of ∼112 cm^{-1} is ascribed to the μ:η^1:η^1-*syn-syn* bidentate coordination of phthalates.[51−53] The FTIR spectra of **1−3** are presented in Figures S6−S8 of the Supporting Information.

Electronic Absorption Spectroscopy. UV−vis spectra of **1−3** measured in MeOH solution are illustrated in Figures S9−S11 of the Supporting Information. All three complexes show multiple bands in the range of 200−900 nm. The broad d−d absorption bands, with maxima at 686 nm (ε = 281 M^{-1} cm^{-1}), 725 nm (ε = 122 M^{-1} cm^{-1}), and 729 nm (ε = 95 M^{-1} cm^{-1}) for **1−3**, respectively, are induced by the $Hcpdp^{2-}$/$cpdp^{3-}$ ligand. These d−d transitions are consistent with copper(II) ions coordinated by oxygen and nitrogen donor atoms of the ligands.[54−56] The intense absorptions bands at 260 nm (ε = 3189 M^{-1} cm^{-1}) and 230 nm (ε = 7307 M^{-1} cm^{-1}), 259 nm (ε = 10060 M^{-1} cm^{-1}) and 230 nm (ε = 11354 M^{-1} cm^{-1}), and 263 nm (ε = 7856 M^{-1} cm^{-1})^{sh} and 230 nm (ε = 11878 M^{-1} cm^{-1}) are dominated by copper(II) ion-bound intraligand π−π* transitions for **1−3**, respectively. For comparison, the UV−vis spectrum of the free ligand H_3cpdp in MeOH has been included, which exhibits three very strong absorption bands at 254 nm (ε = 218835 M^{-1} cm^{-1})^{sh}, 261 nm (ε = 240441 M^{-1} cm^{-1}), and 268 nm (ε = 182728 M^{-1} cm^{-1})^{sh} in the charge-transfer region (Figure S12 of the Supporting Information). The bands at 254 nm (ε = 218835 M^{-1} cm^{-1})^{sh} and 268 nm (ε = 182728 M^{-1} cm^{-1})^{sh} disappear upon coordination with copper(II) ions, with the generation of a new band at 230 nm (ε = 10180 M^{-1} cm^{-1}) in all three complexes. The observed electronic absorption spectral data suggest that the ligand-bound copper(II) assemblies **1−3** remain intact in solution.

https://doi.org/10.1021/acsomega.2c04627
ACS Omega 2022, 7, 39985−39997

Scheme 3. Schematic Pathways for the Synthesis of Complexes 1−3

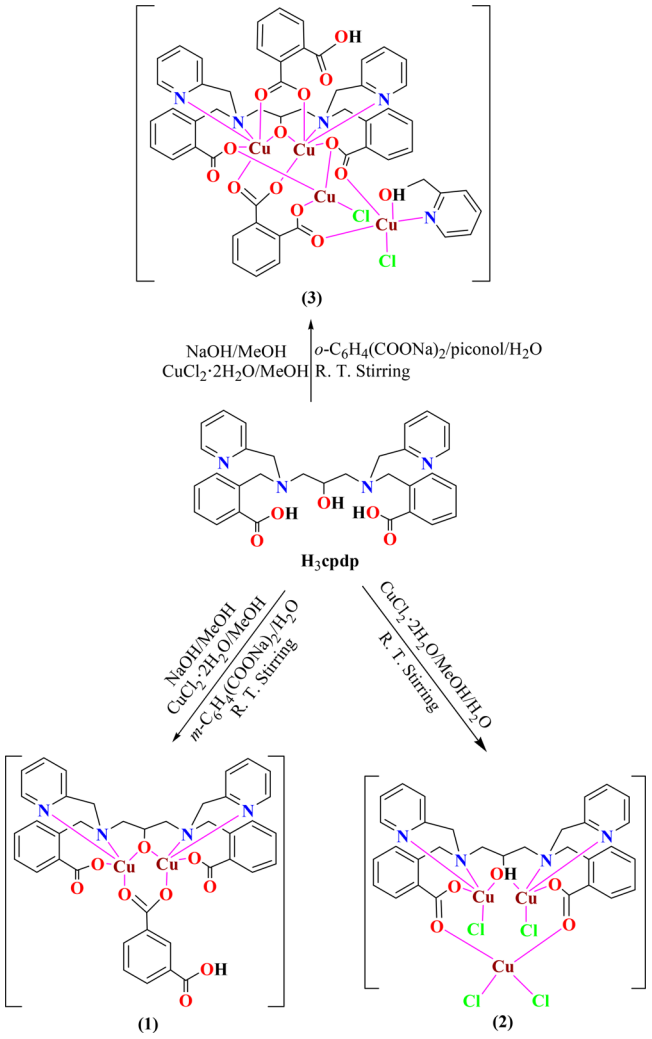

Magnetic Measurements. The molar magnetic susceptibilities (χ_M) of $[Cu_2(cpdp)(\mu\text{-Hisophth})]_4{\cdot}2H_2isophth{\cdot}21H_2O$ (**1**), $[Cu_3(Hcpdp)(Cl)_4]$ (**2**), and tetranuclear $[Cu_4(cpdp)(\mu\text{-Hphth})(\mu_4\text{-phth})(piconol)(Cl)_2]{\cdot}3H_2O$ (**3**) were obtained as 8.831×10^{-3}, 3.138×10^{-3} and 4.809×10^{-3}, respectively, by applying the proper corrections (Pascal's constants) for the diamagnetic components of the ligands and associated ions. Then, by using Gouy methods,[57,58] the magnetic moment values of 1.62 μ_B/Cu (μ_{total} = 4.58 μ_B/Cu_8), 1.58 μ_B/Cu (μ_{total} = 2.73 μ_B/Cu_3), and 1.69 μ_B/Cu (μ_{total} = 3.38 μ_B/Cu_4) for **1**−**3**, respectively, at T = 297 K were determined. The room-temperature magnetic moments lying between 1.58 and 1.69 μ_B correspond to one unpaired electron in each Cu(II) ion. These values are comparable to those reported for analogous copper(II) complexes with μ-alkoxide and exogenous bridging carboxylate groups[59,60] and slightly lower than the spin-only magnetic moment value of 1.73 μ_B/Cu (μ_{total}: 4.89 μ_B/Cu_8 for **1**; 2.99 μ_B/Cu_3 for **2**; 3.46 μ_B/Cu_4 for **3**) expected for eight, three, and four uncoupled spins of Cu(II) ions with S = 1/2 for **1**−**3**, respectively, indicating antiferromagnetic interactions among the paramagnetic copper centers.

Description of Single-Crystal X-ray Structures of 1−3. The single-crystal X-ray technique was employed to establish the molecular structures of all three complexes. Whereas **1** and **2** crystallize in the monoclinic space groups $P2_1$ and $P2_1/m$, respectively, **3** crystallizes in the orthorhombic space group $P2_12_12_1$. Data collection, including crystal and refinement parameters for **1**−**3**, are summarized in Table 1. Selected bond distances and angles for **1**−**3** are given in Tables S1−S3. The views of molecular structures and core frameworks of **1**−**3** were created using Diamond (version 4.0).[61]

*$[Cu_2(cpdp)(\mu\text{-Hisophth})]_4{\cdot}2H_2isophth{\cdot}21H_2O$ (**1**).* The single-crystal X-ray structure of **1** contains four molecules in the asymmetric unit, with equivalent structures of the formula $[Cu_2(cpdp)(\mu\text{-Hisophth})]$, along with two isophthalic acid moieties and 21 lattice waters. A view of the neutral dinuclear $[Cu_2(cpdp)(\mu\text{-Hisophth})]$ complex, together with the atomic numbering scheme, is shown in Figure 1. In each $[Cu_2(cpdp)(\mu\text{-Hisophth})]$ unit, the deprotonated ligand $cpdp^{3-}$ acts as a dinucleating ligand coordinated to the two copper(II) ions. Both copper(II) ions adopt a five-coordinate distorted-square-pyramidal geometry, each provided by one bridging alkoxide oxygen, one benzoate oxygen, one tertiary amine nitrogen, and one pyridine nitrogen of the $cpdp^{3-}$ ligand and the bridging isophthalate group. The values of the Addison parameter (τ)[62] of copper(II) are 0.348 (Cu1A) and 0.167 (Cu2A), suggesting that the geometry around each metal center is highly distorted square pyramidal. Cu1A and Cu2A are shifted by 0.199 and 0.214 Å from the O7AO3AN2AN1A and O6AO3AN4AN3A basal planes, respectively. The alkoxide bridge is asymmetric with two Cu−$O_{alkoxide}$ bond distances differing by about 0.054 Å.

The exogenous isophthalate group connects two copper centers in a $\mu{:}\eta^1{:}\eta^1$-*syn-syn* bidentate fashion. The Cu−$O_{bridging\ isophthalate}$ bond distances specify that this bridge is also asymmetric (Cu1A−O7A, 2.032(6) Å; Cu2A−O6A, 2.003(6) Å). The bond distances to the oxygen and nitrogen atoms around the copper centers are in the range of 1.854(8)−2.247(4) Å, which agree well with those of related dicopper(II) complexes.[63,64] The significant difference in the C39A−O8A and C39A−O9A bond distances (C39A−O8A, 1.24(1) Å; C39A−O9A, 1.33(2) Å), indicate that the C39A−O9A bond is formally a C−OH connection. The location of the hydrogen atoms attached to the oxygen atoms of the carboxylate groups was verified by the difference Fourier map, which is further supported by the inhomogeneous C−O bond distances of the −COOH group. In general, for the −COOH group, the shorter C−O bond may be assigned to a C═O bond, while the longer C−O bond may be assigned to C−OH bond. The Cu1A···Cu2A internuclear separation is 3.437(1) Å, which is in agreement with the distances found in reported dicopper(II) complexes.[65,66]

Figure 2 displays a unit cell packing diagram showing the benzoate, isophthalate and lattice water-susceptible extensive hydrogen bonding interactions that provide the overall stabilization to the crystal lattice. In addition , the adjacent benzoate and pyridyl functions are aligned in a face-to-face orientation with an average centroid-to-centroid distance of ∼3.607 Å, indicating the presence of sensible intramolecular $\pi\cdots\pi$ stacking interactions (Figure 3).

*$[Cu_3(Hcpdp)(Cl)_4]$ (**2**).* A view of the single-crystal X-ray structure of **2** with the atom-numbering scheme is shown in Figure 4. It consists of three copper(II) ions, one $Hcpdp^{2-}$ ligand, and four chloride ions. The structure of **2** can be viewed as a trimetallic assemblage that contains an unsymmetrical $Cu_3O_5N_4Cl_4$ core, with each copper(II) ion located at the corners of an isosceles triangle (Figure 5). The formation of **2**

https://doi.org/10.1021/acsomega.2c04627
ACS Omega 2022, 7, 39985−39997

Table 1. Single-Crystal X-ray Data for $[Cu_2(cpdp)(\mu\text{-Hisophth})]_4{\cdot}2H_2isophth{\cdot}21H_2O$ (1), $[Cu_3(Hcpdp)(Cl)_4]$ (2), and $[Cu_4(cpdp)(\mu\text{-Hphth})(\mu_4\text{-phth})(piconol)(Cl)_2]{\cdot}3H_2O$ (3)

	1	2	3
empirical formula	$C_{172}H_{190}N_{16}O_{65}Cu_8$	$C_{31}H_{30}N_4O_5Cl_4Cu_3$	$C_{53}H_{51}N_5O_{17}Cl_2Cu_4$
formula wt	4029.86	871.05	1355.11
cryst syst	monoclinic	monoclinic	orthorhombic
space group	$P2_1$	$P2_1/m$	$P2_12_12_1$
a, Å	13.1937(2)	7.8680(5)	12.33866(11)
b, Å	21.5249(3)	18.9914(11)	19.5274(2)
c, Å	32.8517(4)	13.1824(8)	22.0140(2)
α, deg	90	90	90
β, deg	92.944(1)	90.599(6)	90
γ, deg	90	90	90
V, Å^3	9317.3(2)	1969.6(2)	5304.11(9)
Z	2	2	4
density, Mg/m^3	1.437	1.469	1.697
wavelength, Å	1.54184	0.71073	1.54184
temp, K	100(10)	100(2)	100(10)
$F(000)$	4156.305	881.613	2739.409
abs coeff, mm^{-1}	1.758	1.916	3.408
θ range, deg	2.460−66.222	3.570−29.050	3.030−66.470
no. of rflns collected	26096	4287	9165
no. of indep rflns	24524	3060	9003
R1 ($I > 2\sigma(I)$)[a]	0.088	0.0834	0.034
Rw (F^2 all data)[a]	0.2456	0.2336	0.0977
goodness of fit on F^2	1.0489	1.0497	1.0537
largest diff peak and hole, e/Å^3	+2.1000, −2.0420	+3.2620, −1.4208	+1.1669, −0.5004

[a] $R1 = \sum||F_o| - |F_c||/\sum|F_o|$; $wR2 = \{\sum[w(F_o^2 - F_c^2)^2]/\sum[w(F_o^2)^2]\}^{1/2}$.

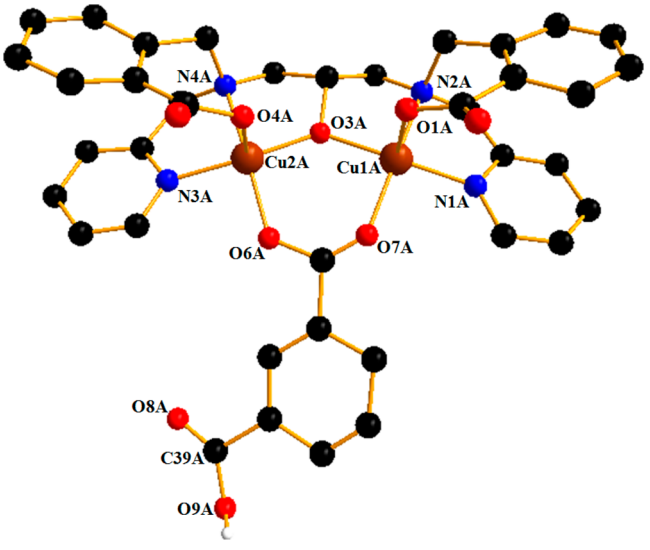

Figure 1. Diamond representation of the molecular structure of $[Cu_2(cpdp)(\mu\text{-Hisophth})]$ in 1 with the atom-numbering scheme. Hydrogen atoms and lattice solvent molecules are omitted for clarity. Color code: Cu, brown; N, blue; O, red; C, black (Diamond - Crystal and Molecular Structure Visualization; Version 4.0).

is accomplished by the self-assembly of a dinuclear $[Cu_2(Hcpdp)]^{2+}$ and a mononuclear $[CuCl_2]$ species which are exclusively bridged by two benzoates in a $\mu{:}\eta^1{:}\eta^1$-*syn-anti* bidentate manner. Within the dinuclear $[Cu_2(Hcpdp)]^{2+}$ unit, the two copper centers show identical coordination geometries, bond distances, and angles. As shown in Figure 5, Cu1 and Cu1′ adopt a distorted-square-pyramidal geometry (τ = 0.079),[62] with each surrounded by one bridging alcohol

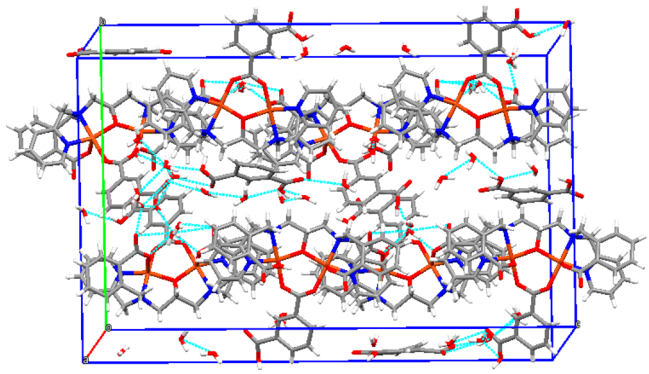

Figure 2. Unit cell packing diagram of 1 showing hydrogen-bonding interactions.

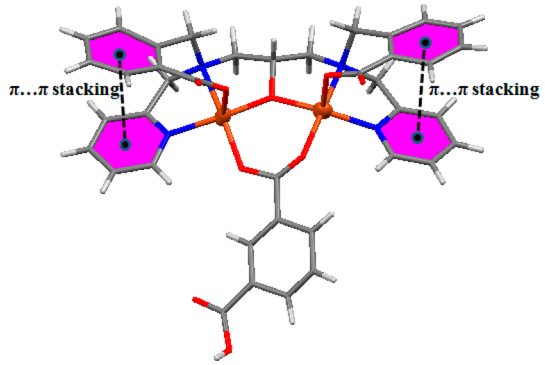

Figure 3. Perspective view of 1 showing intramolecular $\pi\cdots\pi$ stacking interactions.

https://doi.org/10.1021/acsomega.2c04627
ACS Omega 2022, 7, 39985−39997

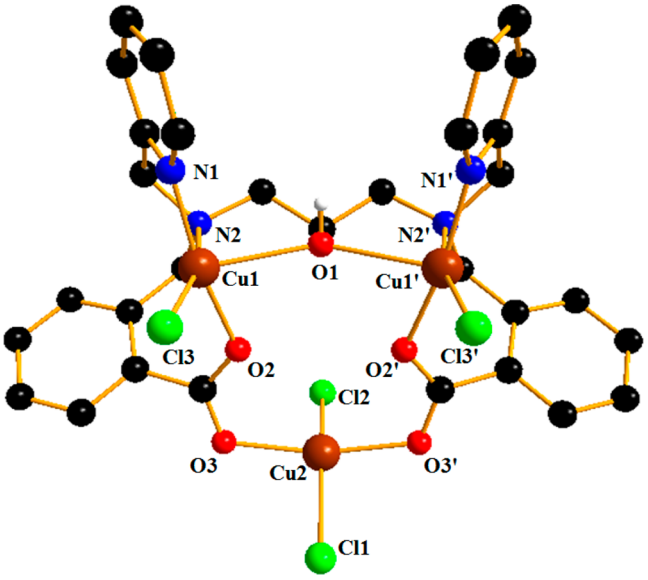

Figure 4. Diamond representation of the molecular structure of $[Cu_3(Hcpdp)(Cl)_4]$ in **2** with the atom-numbering scheme. Hydrogen atoms are omitted for clarity. Color code: Cu, brown; N, blue; O, red; Cl, green; C, black (Diamond - Crystal and Molecular Structure Visualization; Version 4.0).

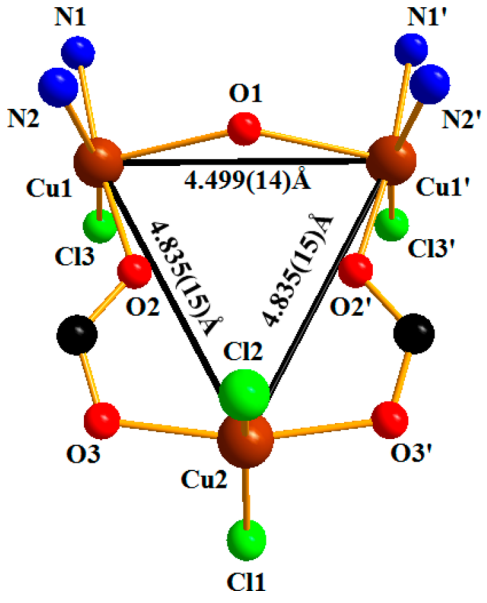

Figure 5. Diamond representation of the core framework of **2** with the atom-numbering scheme showing three copper centers at the corners of an isosceles triangle. Hydrogen atoms are omitted for clarity. Color code: Cu, brown; N, blue; O, red; Cl, green; C, black (Diamond - Crystal and Molecular Structure Visualization; Version 4.0).

oxygen, one bridging benzoate oxygen, one tertiary amine nitrogen, and one pyridine nitrogen of the $Hcpdp^{2-}$ ligand and one exogenous Cl^- ion. In contrast, the geometry around the Cu3 center can be best described as a distorted square plane, completed by two bridging benzoate oxygens and two monodentate Cl^- ions. In order to balance the total charge in **2**, one proton has been added to the O1 atom (alkoxide oxygen). This is further supported by significantly longer Cu1−O1/Cu1′−O1 bond distances of 2.351 Å. The deviations of the Cu1/Cu1′ and Cu3 centers from the O2N2N1Cl3/O2′N2′N1′Cl3′ and O3Cl2Cl1O3′ basal planes are detected as 0.076 and 0.154 Å, respectively. In the $[Cu_3]$ unit, the three copper centers come together at the corners of an isosceles triangle with the edges of 4.835(15), 4.835(15), and 4.499(14) Å (Figure 5). The Cu−O, Cu−N, and Cu−Cl bond distances are in the respective ranges of 1.957(5)−2.351(3), 1.965(6)−2.070(6), and 2.232(3)−2.242(4) Å, which are consistent with literature values.[67,68] As expected, there is no direct covalent linkage among the three copper(II) ions, which are separated by a distance of 4.723 Å (average).[69]

*$[Cu_4(cpdp)(\mu\text{-Hphth})(\mu_4\text{-phth})(piconol)(Cl)_2]\cdot 3H_2O$ (**3**).* A single-crystal X-ray structure analysis reveals that **3** consists of four copper(II) ions, one $cpdp^{3-}$ ligand, one monoanionic and one dianionic phthalate moiety, one piconol, and two chloride ions. Three water molecules cocrystallized with the complex. A view of the molecular structure of **3** is depicted in Figure 6. The tetranuclear $[Cu_4]$ motif is formed through the

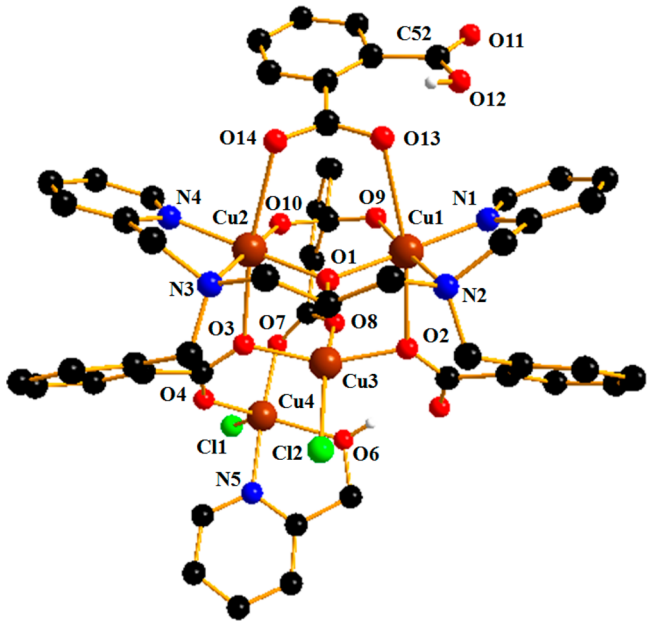

Figure 6. Diamond representation of the molecular structure of $[Cu_4(cpdp)(\mu\text{-Hphth})(\mu_4\text{-phth})(piconol)(Cl)_2]$ in **3** with atom-numbering scheme. Hydrogen atoms are omitted for clarity. Color code: Cu, brown; N, blue; O, red; Cl, green; C, black (Diamond - Crystal and Molecular Structure Visualization; Version 4.0).

aggregation of one dinuclear $[Cu_2(cpdp)]^+$ and two mononuclear $[Cu(piconol)Cl]^+$ and $[CuCl]^+$ units, which are connected to each other by one $\mu{:}\eta^2$ and one $\mu_3{:}\eta^2{:}\eta^1{:}\eta^1$ benzoate group of the $cpdp^{3-}$ ligand as well as one $\mu{:}\eta^1{:}\eta^1$ and one $\mu_4{:}\eta^1{:}\eta^1{:}\eta^1{:}\eta^1$ phthalate group in a *syn-syn* fashion. Within the dinuclear $[Cu_2(cpdp)]^+$ unit, each copper ion (Cu1 and Cu2) exhibits a highly distorted octahedral geometry provided by a bridging alkoxide oxygen, a bridging benzoate oxygen, a tertiary amine nitrogen, a pyridine nitrogen from the $cpdp^{3-}$ ligand, and two bridging carboxylate oxygens from μ- and μ_4-phthalates. Whereas the Cu3 center of the mononuclear $[CuCl]^+$ species shows a distorted-square-planar geometry surrounded by two bridging benzoate oxygens from the $cpdp^{3-}$ ligand, one bridging carboxylate oxygen from the μ_4-phthalate, and one Cl^- ion, the Cu4 center of the mononuclear $[Cu(piconol)Cl]^+$ species adopts a distorted-trigonal-bipyramidal geometry (τ = 0.845)[62] encircled by a bridging

https://doi.org/10.1021/acsomega.2c04627
ACS Omega 2022, 7, 39985−39997

benzoate oxygen from the $cpdp^{3-}$ ligand, a bridging carboxylate oxygen from the μ_4-phthalate, one Cl^- ion, and one pyridine nitrogen and one alcohol oxygen from piconol. A view of the core framework of **3** that shows three different coordination geometries around the copper centers is presented in Figure 7. The O2−Cu3−O8, O2−Cu3−Cl2, O3−Cu3−Cl2, and O8−Cu3−O3 bond angles around the square-planar Cu3 center are 87.65(10), 95.57(8), 94.64(8), and 95.57(10)°, respectively. The Cu1, Cu2, Cu3, and Cu4 centers are displaced by 0.073, 0.016, 0.008, and 0.148 Å from the N2N1O9O1, N4N3O1O10, O2O8O3Cl2, and O4Cl1O6 basal planes, respectively. The $Cu-O_{bridging\ alkoxide}$ bond distances indicate that this bridge is close to symmetrical (Cu1−O1, 1.927(2) Å; Cu2−O1, 1.932(2) Å). The Cu−O, Cu−N, and Cu−Cl bond distances are in agreement with those of analogous copper(II) complexes reported in the literature.[67,68] The longer C52−O12 bond, having a distance of 1.305(7) Å, is formally a C−OH linkage specified by the proton position to be found in the difference Fourier map. This observation agrees well with the inhomogeneous C−O bond distances of the −COOH group. Generally, for the −COOH group, the shorter C−O bond may be assigned to a C═O bond, while the longer C−O bond may be assigned to a C−OH bond. The intraligand Cu1···Cu2 separation is 3.4510(6) Å.[65,66]

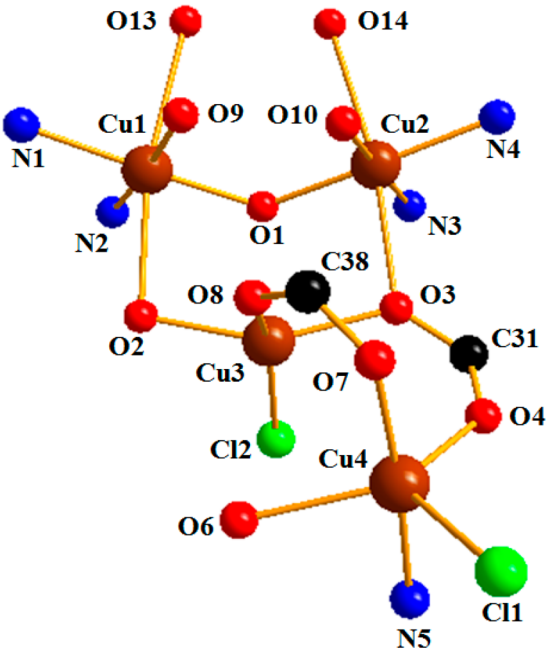

Figure 7. Diamond representation of the core framework of **3** with atom-numbering scheme. Hydrogen atoms are omitted for clarity. Color code: Cu, brown; N, blue; O, red; Cl, green; C, black (Diamond - Crystal and Molecular Structure Visualization; Version 4.0).

Although the bidentate $\mu:\eta^2$ and $\mu:\eta^1:\eta^1$ bridging modes are quite common in metal carboxylate coordination chemistry, the simultaneous existence of both tridentate $\mu_3:\eta^2:\eta^1:\eta^1$ and tetradentate $\mu_4:\eta^1:\eta^1:\eta^1:\eta^1$ bridging modes is rare.[34,46,70] Hence, **3** is an unprecedented example of a tetranuclear copper(II) complex that exhibits the bidentate $\mu:\eta^2$ and $\mu:\eta^1:\eta^1$, tridentate $\mu_3:\eta^2:\eta^1:\eta^1$, and tetradentate $\mu_4:\eta^1:\eta^1:\eta^1:\eta^1$ bridging modes of the carboxylate groups concurrently, linking four copper centers. A careful search of the data in the literature shows that complex **3** is the third example of a structurally characterized μ_4-phthalate-bridged metal complex. Very recently, only the $[Cr_4Ln_4]$ cluster, incorporating a trilacunary Keggin-type polyoxometalate, and an Mn_5 cluster with a "twisted bow-tie" topology that are stabilized by phthalate groups showing $\mu_4:\eta^1:\eta^1:\eta^1:\eta^1$ bridging modes have been reported.[71] Hence, to our knowledge, complex **3** is the first crystallographically characterized solid-state structure of a Cu(II) complex of any nuclearity where a doubly deprotonated phthalate group shows a unique $\mu_4:\eta^1:\eta^1:\eta^1:\eta^1$ bridging mode.

It is notable to state that complex **3** exhibits the benzoate, phthalate, piconol, and lattice water-susceptible wide-ranging H-bond interactions supporting an additional stabilization of the crystal lattice (Figure S13 of the Supporting Information). The moderate intramolecular $\pi\cdots\pi$ stacking interactions are also observed among the adjacent benzoate and pyridyl functions due to their face-to-face array with an average centroid-to-centroid distance of ∼3.949 Å (Figure 8).

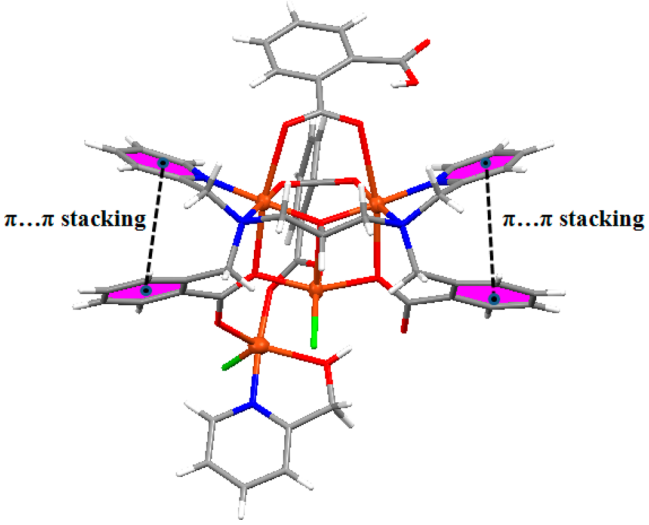

Figure 8. Perspective view of **3** showing intramolecular $\pi\cdots\pi$ stacking interactions.

Structural Comparison of Complexes 1−3. Structural features, including the coordination properties, of **1**−**3** have been compared with respect to their supramolecular assemblies. Whereas **1** and **2** represent a μ-alkoxide/alcohol and μ-carboxylate-bridged dimeric Cu_2 and trimeric Cu_3 complexes, **3** embodies a μ-alkoxide- and μ-, μ_3-, and μ_4-carboxylate-bridged tetrameric Cu_4 complex. Complex **1** is formed through the self-assembly of two Cu(II) ions, one fully deprotonated $cpdp^{3-}$ ligand, and one monoanionic isophthalate group; complex **2** is produced by the self-assembly of a dinuclear $[Cu_2(Hcpdp)]^{2+}$ and a mononuclear $[CuCl_2]$ species which are exclusively connected by two benzoate groups; complex **3** is fashioned through the self-assembly of one dinuclear $[Cu_2(cpdp)]^+$ and two mononuclear [Cu(piconol)-Cl]$^+$ and $[CuCl]^+$ species that are linked to each other by two benzoate groups as well as one monoanionic and one dianionic phthalate group. While complex **1** shows monodentate terminal coordination in relation to endogenous benzoate groups and $\mu:\eta^1:\eta^1$-*syn-syn* bidentate coordination in relation to an exogenous isophthalate group and complex **2** displays $\mu:\eta^1:\eta^1$-*syn-anti* bidentate coordination concerning the endog-

https://doi.org/10.1021/acsomega.2c04627
ACS Omega 2022, 7, 39985−39997

enous benzoate groups, complex **3** exhibits μ:η^2 bidentate and μ_3:η^2:η^1:η^1 tridentate bridging modes with respect to endogenous benzoate groups as well as the μ:η^1:η^1 bidentate and μ_4:η^1:η^1:η^1:η^1 tetradentate bridging modes with respect to exogenous phthalate groups. Furthermore, the prominent structural features of their crystal structures also lie in the coordination geometries around the Cu(II) ions, which are markedly different. In **1**, the two Cu(II) ions assume a distorted-square-pyramidal geometry; in **2**, two Cu(II) ions adopt a distorted-square-pyramidal geometry and the other Cu(II) ion adopts a distorted-square-planar geometry; in **3**, two Cu(II) ions exhibit a distorted-octahedral geometry, one Cu(II) ion exhibits a distorted-trigonal-bipyramidal geometry, and the other Cu(II) ion shows a distorted-square-planar geometry. Careful analyses of X-ray crystal structures show that the average Cu···Cu distances of 3.437, 4.723, and 3.383 Å in **1**−**3**, respectively, are significantly longer than the sum of the covalent radii of two coppers of 2.8 Å (r_{cov} = 1.4 Å), and hence, there is no direct Cu···Cu interaction.[72] Evidently, the different Cu···Cu distances are caused by the various structural diversities which are due to the different coordination modes of the organic ligands. While the occurrence of plentiful hydrogen-bonding interactions and moderate intramolecular π···π stacking interactions observed in **1** and **3** contribute toward the stabilization of their crystal lattices, both the hydrogen-bonding and π···π stacking interactions are absent in **2**. The π···π stacking interaction is a kind of attractive and noncovalent interaction that occurs when the aromatic π-systems interact face-to-face with one another and involves a combination of dispersion and dipole-induced dipole interactions.[73] In fact, aromaticity should be an essential requirement for the occurrence of π···π stacking interactions. In line with this, the intramolecular π···π stacking interactions are detected in **1** and **3** due to face-to-face arrangements of adjoining pyridyl and benzoate moieties with average centroid-to-centroid distances of 3.607 and 3.949 Å, respectively. In comparison to the model porphyrin−porphyrin interactions (3.4 Å),[74] the observed π···π stacking interactions can be classified as moderate interactions. Considering the aforementioned striking structural features, it can be seen that **1**−**3** are interesting examples of a family of self-assembled di-, tri-, and tetranuclear copper(II) complexes of a symmetrical dinucleating ligand, showing several versatile and rare coordination/binding modes of carboxylates with unsymmetrical arrangements of Cu(II) ions, particularly in **2** and **3**.

Powder X-ray Diffraction Studies. Powder X-ray diffraction experiments (PXRD) were performed for **1**−**3** using their microcrystalline samples obtained upon drying in a vacuum desiccator. The PXRD patterns of **1**−**3** are shown in Figures S14−S16 of the Supporting Information, respectively. The PXRD patterns for all three complexes are consistent with the simulated patterns acquired from the single-crystal X-ray diffraction data. The PXRD patterns also indicate that their peak positions are in good agreement with each other, suggesting the phase purity of the complexes. Nevertheless, for all three complexes, there are small differences in the peak intensities of experimental and simulated patterns, which may be due to the preferred orientation of the power.

Thermal Properties. The thermal analyses (TGA/DTA) data for **1**−**3** are given in Figures 9−11. Complex **1** is thermally stable up to ∼213 °C. In the temperature interval of 81−121 °C, the TGA curve of **1** indicates a first mass loss of ∼9.63% (calcd 9.39%), which can be attributed to the loss of

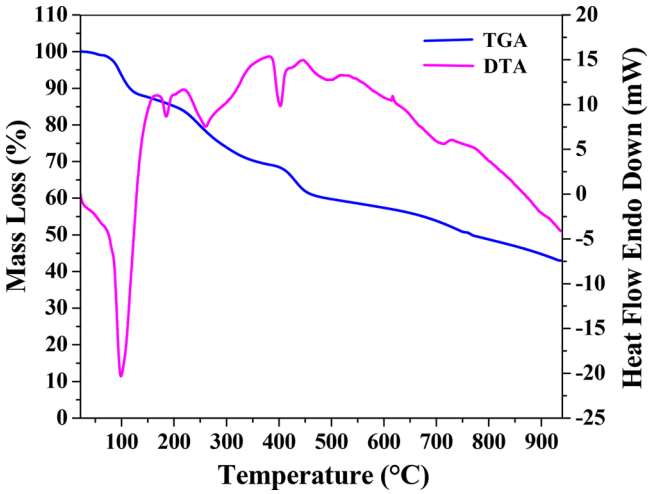

Figure 9. TGA/DTA profiles of **1** under an inert atmosphere of N_2 gas with a heating rate of ∼10 °C/min.

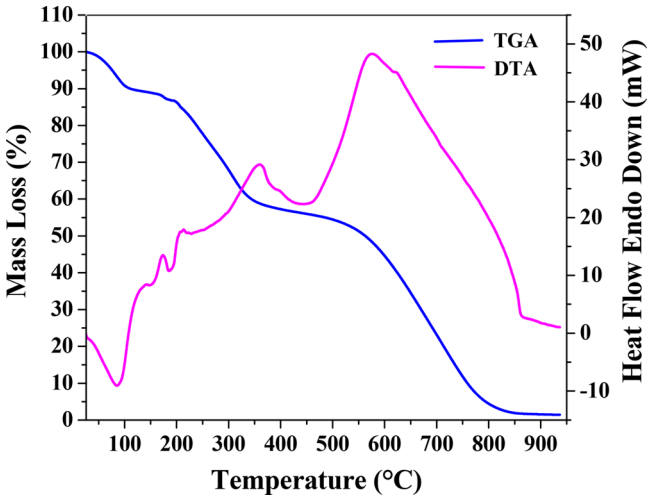

Figure 10. TGA/DTA profiles of **2** under an inert atmosphere of N_2 gas with a heating rate of ∼10 °C/min.

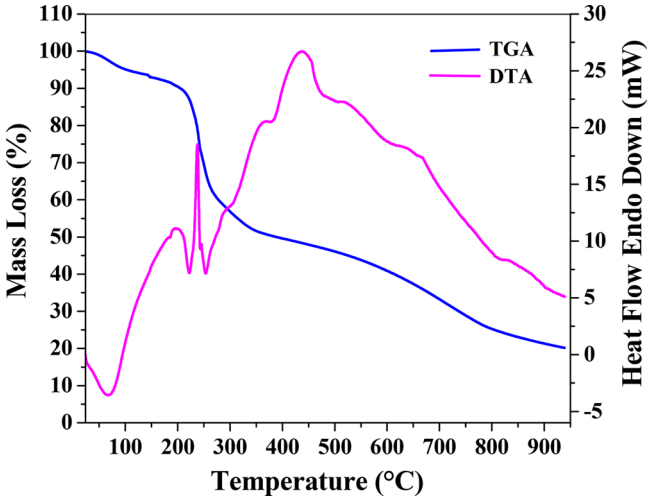

Figure 11. TGA/DTA profiles of **3** under an inert atmosphere of N_2 gas with a heating rate of ∼10 °C/min.

21 lattice H_2O molecules. The corresponding DTA curve shows a strong endothermic effect with a peak minimum

https://doi.org/10.1021/acsomega.2c04627
ACS Omega 2022, 7, 39985−39997

temperature (T_{min}) of 99 °C. The second decomposition step associated with a mass loss of ∼4.16% (calcd 4.36%) is due to the release of four CO_2 gas molecules between 128 and 212 °C from two free isophthalic acids. The third and fourth decomposition steps in the temperature interval of 213−411 °C account for the total mass losses of ∼17.05% (calcd 17.47%) indicating the release of 16 CO_2 gas molecules from four coordinated $cpdp^{3-}$ and four coordinated isophthalates. In connection with these three decarboxylation processes, the DTA curve exhibits three weak endothermic peaks with T_{min} at 185, 259, and 402 °C. Afterward, complex **3** shows the decomposition of the metal−organic framework through two-step thermal processes between 415 and 950 °C, accompanied by the consequent DTA peaks with T_{min} at 494 °C (weak endothermic) and 712 °C (weak endothermic). Complex **2** is thermally stable up to ∼242 °C. In the temperature interval of 47−97 °C, the TGA curve of **2** shows a first mass loss of ∼8.03% (calcd 8.15%), corresponding to the removal of a Cl_2 gas molecule. The consequent DTA curve displays an endothermic effect with T_{min} at 86 °C. In the second step, the mass loss of ∼8.34% (calcd 8.15%) between 172 and 242 °C is attributed to the removal of another Cl_2 gas molecule exhibiting the corresponding DTA curve that shows a weak endothermic peak with T_{min} at 188 °C. The expulsion of two Cl_2 gas molecules in two different temperature windows is most probably due to different electronic effects experienced by the chloride ions coordinated to the distorted-square-pyramidal and distorted-square-planar copper centers. After that, the decomposition of the metal−organic framework occurs between 243 and 825 °C, including the loss of two CO_2 gas molecules at ∼292 °C. The resultant DTA peaks show a weak and strong exothermic effects with peak maxima (T_{max}) at 360 and 577 °C, respectively. Complex **3** is thermally stable up to ∼211 °C. The TGA curve of **3** shows a first mass loss of ∼3.80% (calcd 3.98%) in the temperature interval of 50−98 °C that corresponds to a loss of three lattice waters, followed by the expulsion of a Cl_2 gas molecule between 100 and 209 °C in the second step, indicating a mass loss of ∼5.45% (calcd 5.23%). The corresponding DTA curve shows two endothermic peaks with T_{min} at 67 and 222 °C. Subsequently, the decomposition of the metal−organic framework occurs between 211 and 810 °C, including the removal of six CO_2 gas molecules at ∼250 °C. As a consequence, the DTA peaks with T_{min} at 255 °C (strong endothermic) and T_{max} at 362 °C (weak exothermic), 436 °C (strong exothermic), 526 °C (weak exothermic), and 642 °C (weak exothermic) associated with the multistep thermal decomposition processes are observed. The leftover masses correspond to the formation of CuO as the possible final residue for all three complexes.[75,76] Comparable thermal behavior has been reported in the literature, showing the removal of lattice H_2O, Cl_2, and CO_2 gases from allied chloride-/carboxylate-containing metal complexes.[77−79]

CONCLUSION

In conclusion, the symmetrical dinucleating ligand H_3cpdp, in combination with exogenous ancillary ligands such as isophthalate, chloride, and phthalate/chloride/piconol, yields a new family of di-, tri-, and tetranuclear copper(II) complexes under the specified experimental conditions. All three complexes have been characterized by single-crystal X-ray studies, which disclose that their metallic core arrangements are distinctly different from each other. From the structural analyses the important role played by the exogenous ancillary ligands in synthesizing and controlling the molecular topology of these copper(II) complexes is obvious. At the outset, the dinucleating ligand H_3cpdp facilitates the trapping of two copper(II) ions, leaving available coordination sites for the binding of isophthalate, chloride, and phthalate/chloride/piconol moieties, which help the assembly of two, three, and four copper(II) ions in the final molecular architectures of **1**−**3**, respectively. Most importantly, complexes **2** and **3** unveil fascinating coordination chemistry, with a trimeric $[Cu_3]$ core in which a dinuclear $[Cu_2(Hcpdp)]^{2+}$ species is entirely linked to a mononuclear $[CuCl_2]$ species by two μ:η^1:η^1-*syn-anti* carboxylate groups having a triangular design in **2** and with a tetrameric $[Cu_4]$ core in which one dinuclear $[Cu_2(cpdp)]^+$ and two mononuclear $[Cu(piconol)Cl]^+$ and $[CuCl]^+$ species are connected to each other by one μ:η^2 benzoate, one μ_3:η^2:η^1:η^1 benzoate, one μ:η^1:η^1 phthalate, and one μ_4:η^1:η^1:η^1:η^1 phthalate group in **3**. It is important to mention that **3** is a rare example of a copper(II)-based tetranuclear complex that displays multifaceted coordination modes of carboxylates, with an unprecedented μ_4:η^1:η^1:η^1:η^1 bridging coordination mode of the phthalate group. The thermal behavior of **1**−**3** has been examined by TGA/DTA techniques, indicating that the complexes are stable up to ∼208 °C (average). Magnetic studies of **1**−**3** at room temperature show the sensible antiferromagnetic interactions among the copper(II) ions. The interesting and versatile coordination phenomena of carboxylate-based ligands with Cu(II) exhibiting multiple coordination geometries discussed in the present article will positively contribute to the field of supramolecular coordination chemistry.

EXPERIMENTAL SECTION

Materials. The chemicals used were obtained from the following sources: 2-carboxybenzaldehyde, 2-picolyl chloride hydrochloride, 1,3-diamino-2-propanol, 2-pyridinemethanol, sodium borohydride, and lithium hydroxide from Sigma-Aldrich, Germany; copper(II) chloride dihydrate and sodium hydroxide from SRL, India; sodium phthalate and sodium isophthalate from TCI, USA. All other chemicals and solvents were reagent-grade materials and were used as received without further purification.

Synthesis of H_3cpdp. The ligand H_3cpdp was synthesized and characterized as reported by us previously.[45] The composition of the ligand was ascertained by elemental analysis, NMR spectroscopy, mass spectrometry, and thermogravimetric analysis. Yield: 4.018 g (77%).

Synthesis of $[Cu_2(cpdp)(\mu\text{-Hisophth})]_4\cdot 2H_2$isophth$\cdot 21H_2O$ (1). $CuCl_2\cdot 2H_2O$ (0.157 g, 0.92 mmol) dissolved in methanol (8 mL) was added dropwise with stirring to a methanol solution (10 mL) of H_3cpdp (0.511 g, 0.46 mmol) and NaOH (0.055g, 1.38 mmol). The bluish green solution that formed was stirred for 1 h. After that, *m*-$C_6H_4(CO_2Na)_2$ (0.096 g, 0.46 mmol) in 2 mL of water was added slowly and the stirring was continued for another 1 h. The pH of the final bluish green solution was checked to be ∼6.5. The solution was filtered, and bluish green single crystals suitable for X-ray analysis were grown from the clear filtrate by diffusing diethyl ether after ∼7 days. Yield: 0.305 g (65%). Anal. Calcd for $C_{172}H_{190}N_{16}O_{65}Cu_8$: C, 51.26%; H, 4.75%; N, 5.56%; Cu, 12.62%. Found: C, 51.35%; H, 4.88%; N, 5.61%; Cu, 12.81%. Molar conductance: Λ_M (MeOH) = 22 Ω^{-1} cm^2 mol^{-1}. FTIR (KBr, cm^{-1}): ν 3401(b), 1609(s), 1553(s), 1481(s), 1447(s),

https://doi.org/10.1021/acsomega.2c04627
ACS Omega 2022, 7, 39985−39997

1377(s), 1287(s), 1153(s), 1105(s), 1074(s), 1051(s), 1032(s), 991(s), 940(s), 856(s), 820(s), 756(s), 715(s), 658(s), 614(s). UV−vis (MeOH): λ_{max}, nm (ε, $M^{-1}cm^{-1}$) 686 (281), 260 (3189), 230 (7307).

Synthesis of $[Cu_3(Hcpdp)(Cl)_4]$ (2). $CuCl_2{\cdot}2H_2O$ (0.235 g, 1.38 mmol) dissolved in methanol (8 mL) was added dropwise with stirring to a methanol solution (10 mL) of H_3cpdp (0.511 g, 0.46 mmol). After about 15 min of stirring, 2 mL of distilled water was added to give a clear green solution. The resulting green solution was further stirred for 1 h. The pH of the final green solution was checked to be ∼3. The solution was filtered, and green single crystals suitable for X-ray analysis were obtained from the clear filtrate by diffusing diethyl ether after ∼5 days. Yield: 0.309 g (76%). Anal. Calcd for $C_{31}H_{30}N_4O_5Cl_4Cu_3$: C, 42.75%; H, 3.47%; N, 6.43%; Cu, 21.89%. Found: C, 42.82%; H, 3.56%; N, 6.19%; Cu, 22.05%. Molar conductance: Λ_M (MeOH) = 18 Ω^{-1} cm^2 mol^{-1}. FTIR (KBr, cm^{-1}): ν 3434(b), 1612(s), 1584(s), 1559(s), 1484(s), 1450(s), 1419(s), 1258(s), 1158(s), 1029(s), 970(s), 870(s), 809(s), 770(s), 722(s), 678(s). UV−vis (MeOH): λ_{max}, nm (ε, $M^{-1}cm^{-1}$) 725 (122), 259 (10060), 230 (11354).

Synthesis of $[Cu_4(cpdp)(\mu\text{-Hphth})(\mu_4\text{-phth})(piconol)(Cl)_2]{\cdot}3H_2O$ (3). $CuCl_2{\cdot}2H_2O$ (0.314 g, 1.84 mmol) dissolved in methanol (8 mL) was added dropwise with stirring to a methanol solution (10 mL) of H_3cpdp (0.511 g, 0.46 mmol) and NaOH (0.055 g, 1.38 mmol). The bluish green solution that formed was stirred for 1 h. Next, o-$C_6H_4(CO_2Na)_2$ (0.193 g, 0.92 mmol) in 2 mL of water was added slowly, followed by the dropwise addition of piconol (0.050 g, 0.46 mmol). The resulting bluish green solution was further stirred for 1 h. The pH of the final solution was checked to be ∼6.5. The solution was filtered, and bluish green single crystals suitable for X-ray analysis were formed from the clear filtrate by diffusing diethyl ether after ∼5 days. Yield: 0.442 g (70%). Anal. Calcd for $C_{53}H_{51}N_5O_{17}Cl_2Cu_4$: C, 46.98%; H, 3.79%; N, 5.17%; Cu, 18.76%. Found: C, 46.79%; H, 4.62%; N, 5.28%; Cu, 18.58%. Molar conductance: Λ_M (MeOH) = 15 Ω^{-1} cm^2 mol^{-1}. FTIR (KBr, cm^{-1}): ν 3408(b), 3078(b), 1615(s), 1564(s), 1485(s), 1452(s), 1420(s), 1367(s), 1285(s), 1151(s), 1107(s), 1024(s), 991(s), 905(s), 853(s), 816(s), 761(s), 713(s), 661(s), 613(s), 534(s), 470(s). UV−vis (MeOH): λ_{max}, nm (ε, $M^{-1}cm^{-1}$) 729 (95), 263 (7856), 230 (11878).

Physical Measurements. Elemental analyses (C, H, N) were performed with a PerkinElmer 2400 CHNS/O Series II elemental analyzer. Analyses of copper contents in the complexes was performed by an iodometric titration method (using $Na_2S_2O_3$) in aqueous solution, after digesting their crystalline powder samples in a concentrated HCl/HNO_3 mixture. NMR spectra of H_3cpdp were obtained with a Bruker AC 400 NMR spectrometer. Fourier transform infrared (FTIR) spectra were recorded on a PerkinElmer L120−000A spectrometer. The solution electrical conductivity and electronic spectra were obtained using a METTLER TOLEDO Five EASY Plus FEP 30 digital conductivity meter with a solute concentration of $\sim10^{-3}$ M and a Shimadzu UV 1800 spectrophotometer, respectively. Magnetic susceptibility studies of the complexes were determined in the solid state with a home-built Gouy balance at room temperature using $Hg[Co(SCN)_4]$ as the calibrant. Diamagnetic corrections were made by using Pascal's constants. The powder X-ray diffraction (PXRD) spectra were obtained using a Rigaku (Mini Flex II, Japan) X-ray diffractometer having Cu Kα = 1.54059 Å radiation with a Bragg angular range of 2θ ($5° < 2\theta < 50°$). Thermal studies were executed with a PerkinElmer Diamond TG/DTA thermal analyzer with a heating rate of 10 °C/min.

Single-Crystal X-ray Data Collection and Structure Determination of 1−3. The X-ray crystallographic data for **1** and **3** were collected at 293 and 100 K, respectively, on a SuperNova, Dual, Cu at zero diffractometer, and X-ray crystallographic data for **2** were collected at 100 K on a Bruker Kappa APEX II Quazar diffractometer. The data for **1** and **3** were collected using Cu Kα radiation (λ = 1.54184 Å), and the data for **2** were collected using Mo Kα radiation (λ = 0.71073 Å). The SAINT[80] package and SADABS[81] program were applied for processing and multiscan empirical absorption corrections of the crystallographic data, respectively. The structures were solved by direct methods using the program SIR-97[82] and refined by full-matrix least squares on F^2 with SHELXL[83] and OLEX2.[84] For **1**, after several attempts of data collection, the reported structure was found to be the best one. As the crystal quality was not good, there are a number of disorders present in the structure. Consequently, the quality of the single-crystal X-ray data and the refined model of **1** were affected by these observed disorders. Several alerts were generated because of these observed disorders in its structure. For **2**, during solving and refining the structure, the quality of X-ray data and refining model were affected by some disorders. It was also observed that the unit cell contains large accessible voids in the crystal structure. Because of these reasons, slightly high residual electron density in its structure was obtained, and no model for any solvent could be detected. The refinement was performed anisotropically using full-matrix least squares with all non-H atoms. The difference Fourier map was used to locate the hydrogen atoms. Hydrogen atoms of the complexes were included in idealized positions (C−H, 0.96 Å) and refined as riding models. The hydroxyl H and water H atoms were located precisely.

■ ASSOCIATED CONTENT

Supporting Information

The Supporting Information is available free of charge at https://pubs.acs.org/doi/10.1021/acsomega.2c04627.

FTIR and ^1H and ^{13}C NMR spectra and TGA curve of H_3cpdp, packing diagram of **3**, FTIR, UV−vis, and PXRD spectra of **1**−**3**, and TGA/DTA curve of **2** (PDF)

Crystallographic details for **1** (CIF)

Crystallographic details for **2** (CIF)

Crystallographic details for **3** (CIF)

■ AUTHOR INFORMATION

Corresponding Author

Manindranath Bera − *Department of Chemistry, University of Kalyani, Kalyani, West Bengal 741235, India;* orcid.org/0000-0001-6230-5756; Phone: +91-33-25828282; Email: mbera2009@klyuniv.ac.in; Fax: +91-33-25828282

Authors

Avishek Majumder − *Department of Chemistry, University of Kalyani, Kalyani, West Bengal 741235, India*

Sujan Sk − *Department of Chemistry, University of Kalyani, Kalyani, West Bengal 741235, India*

Arpan Das − *Department of Chemical Sciences, Indian Institute of Science Education & Research-Kolkata, Mohanpur, West Bengal 741246, India*

https://doi.org/10.1021/acsomega.2c04627
ACS Omega 2022, 7, 39985−39997

Gonela Vijaykumar − *Department of Chemical Sciences, Indian Institute of Science Education & Research-Kolkata, Mohanpur, West Bengal 741246, India;* Present Address: Technische Universität Berlin, Institut für Chemie, C261 Strasse des 17. Juni 135, 10623 Berlin, Germany; orcid.org/0000-0002-1249-7347

Malaya K. Sahoo − *School of Chemical Sciences, National Institute of Science Education & Research, An OCC of Homi Bhabha National Institute, Bhubaneswar, Odisha 752050, India*

J. N. Behera − *School of Chemical Sciences, National Institute of Science Education & Research, An OCC of Homi Bhabha National Institute, Bhubaneswar, Odisha 752050, India;* orcid.org/0000-0003-1161-588X

Complete contact information is available at: https://pubs.acs.org/10.1021/acsomega.2c04627

Notes

The authors declare no competing financial interest.

■ ACKNOWLEDGMENTS

The authors gratefully acknowledge the Department of Science, Technology and Biotechnology, West Bengal, India, for funding and financial support (Grant No. ST/P/S&T/15G-18/2019). The authors also acknowledge the DST-FIST (Level-2; SR/FST/CS-II/2019/96) program for supporting the instrumental facilities at the Department of Chemistry, University of Kalyani. M.B. also acknowledges the financial support received from a personal research grant (PRG) of the University of Kalyani. The contingency grant provided by the DST-PURSE program of University of Kalyani is acknowledged. A.M. and S.S. are also thankful to the UGC, New Delhi, for offering a Senior Research Fellowship and Junior Research Fellowship, respectively.

■ REFERENCES

(1) Alexeev, Y. E.; Kharisov, B. I.; Garcia, T. C. H.; Garnovskii, A. D. Coordination Motifs in Modern Supramolecular Chemistry. *Coord. Chem. Rev.* **2010**, *254*, 794−831.

(2) Chakrabarty, R.; Mukherjee, P. S.; Stang, P. J. Supramolecular Coordination: Self-Assembly of Finite Two- and Three-Dimensional Ensembles. *Chem. Rev.* **2011**, *111*, 6810−6918.

(3) Hiraoka, S. Unresolved Issues That Remain in Molecular Self-Assembly. *Bull. Chem. Soc. Jpn.* **2018**, *91*, 957−978.

(4) Zhou, L. P.; Sun, Q. F. A self-assembled Pd_2L_4 Cage That Selectively Encapsulates Nitrate. *Chem. Commun.* **2015**, *51*, 16767−16770.

(5) Sepehrpour, H.; Fu, W.; Sun, Y.; Stang, P. J. Biomedically Relevant Self-assembled Metallacycles and Metallacages. *J. Am. Chem. Soc.* **2019**, *141*, 14005−14020.

(6) Mukherjee, A.; Rudra, I.; Naik, S. G.; Ramasesha, S.; Nethaji, M.; Chakravarty, A. R. Covalent Linkage of the Type-2 and Type-3 Structural Mimics to Model the Active Site Structure of Multicopper Oxidases: Synthesis and Magneto-Structural Properties of Two Angular Trinuclear Copper(II) Complexes. *Inorg. Chem.* **2003**, *42*, 5660−5668.

(7) Biswas, A.; Drew, M. G. B.; Gómez-García, C. J.; Ghosh, A. Use of a Reduced Schiff-Base Ligand to Prepare Novel Chloro-Bridged Chains of Rare Cu(II) Trinuclear Complexes with Mixed Azido/Oxo and Chloro/Oxo Bridges. *Inorg. Chem.* **2010**, *49*, 8155−8163.

(8) Olson, A. J.; Hu, Y. H.; Keinan, E. Chemical Mimicry of Viral Capsid Self-Assembly. *Proc. Natl. Acad. Sci. U. S. A.* **2007**, *104*, 20731−20736.

(9) Liu, M.; He, Y.; Shan, C.; Wojtas, L.; Ghiviriga, I.; Fathalla, O.; Yan, Y.; Li, X.; Shi, X. Anion Mediated, Tunable Isoguanosine Self-Assemblies: Decoding the Conformation Influence and Solvent Effects. *Chem. Sci.* **2021**, *12*, 7569−7574.

(10) Northrop, B. H.; Zheng, Y. R.; Chi, K. W.; Stang, P. J. Self-Organization in Coordination-Driven Self-Assembly. *Acc. Chem. Res.* **2009**, *42*, 1554−1563.

(11) Sarkar, M.; Clerac, R.; Mathoniere, C.; Hearns, N. G. R.; Bertolasi, V.; Ray, D. New Phenoxido-Bridged Quasi-Tetrahedral and Rhomboidal $[Cu_4]$ Compounds Bearing μ_4-Oxido or $\mu_{1,1}$-Azido Ligands: Synthesis, Chemical Reactivity, and Magnetic Studies. *Inorg. Chem.* **2011**, *50*, 3922−3933.

(12) Sarkar, M.; Clerac, R.; Mathoniere, C.; Hearns, N. G. R.; Bertolasi, V.; Ray, D. New μ_4-Oxido-Bridged Copper Benzoate Quasi-Tetrahedron and Bis-μ_3-Hydroxido-Bridged Copper Azide and Copper Thiocyanate Stepped Cubanes: Core Conversion, Structural Diversity, and Magnetic Properties. *Inorg. Chem.* **2010**, *49*, 6575−6585.

(13) Ghosh, T. K.; Maity, S.; Mayans, J.; Ghosh, A. Family of Isomeric Cu^{II}-Ln^{III} (Ln = Gd, Tb, and Dy) Complexes Presenting Field-Induced Slow Relaxation of Magnetization Only for the Members Containing Gd^{III}. *Inorg. Chem.* **2021**, *60*, 438−448.

(14) Zhang, D.; Ronson, T. K.; Xu, L.; Nitschke, J. R. Transformation Network Culminating in a Heteroleptic $Cd_6L_6L'_2$ Twisted Trigonal Prism. *J. Am. Chem. Soc.* **2020**, *142*, 9152−9157.

(15) Kumar, A.; Zangrando, E.; Mukherjee, P. S. Self-Assembled Pd_3L_2 Cages Having Flexible Tri-imidazole Donors. *Polyhedron* **2019**, *172*, 67−73.

(16) Schneider, J. D.; Smith, B. A.; Williams, G. A.; Powell, D. R.; Perez, F.; Rowe, G. T.; Yang, L. Synthesis and Characterization of Cu(II) and Mixed-Valence Cu(I)Cu(II) Clusters Supported by Pyridylamide Ligands. *Inorg. Chem.* **2020**, *59*, 5433−5446.

(17) Chandrasekhar, V.; Nagarajan, L.; Hossain, S.; Gopal, K.; Ghosh, S.; Verma, S. Multicomponent Assembly of Anionic and Neutral Decanuclear Copper(II) Phosphonate Cages. *Inorg. Chem.* **2012**, *51*, 5605−5616.

(18) Isaac, J. A.; Mansour, A. T.; David, R.; Kochem, A.; Philouze, C.; Demeshko, S.; Meyer, F.; Réglier, M.; Simaan, A. J.; Caldarelli, S.; Yemloul, M.; Jamet, H.; Thibon-Pourret, A.; Belle, C. Tetranuclear and Dinuclear Phenoxido Bridged Copper Complexes Based on Unsymmetrical Thiosemicarbazone Ligands. *Dalton Trans.* **2018**, *47*, 9665−9676.

(19) Ruben, M.; Rojo, J.; Romero-Salguero, F. J.; Uppadine, L. H.; Lehn, J. M. Grid-Type Metal Ion Architectures: Functional Metallosupramolecular Arrays. *Angew. Chem., Int. Ed.* **2004**, *43*, 3644−3662.

(20) Ruben, M.; Lehn, J.-M.; Muller, P. Addressing Metal Centres in Supramolecular Assemblies. *Chem. Soc. Rev.* **2006**, *35*, 1056−1067.

(21) Plass, W. Structural Variety and Magnetic Properties of Polynuclear Assemblies Based on 2-Aminoglucose and Tritopic Triaminoguanidine Ligands. *Coord. Chem. Rev.* **2009**, *253*, 2286−2295.

(22) Kirillov, A. M.; Kirillova, M. V.; Pombeiro, A. J. L. Multicopper Complexes and Coordination Polymers for Mild Oxidative Functionalization of Alkanes. *Coord. Chem. Rev.* **2012**, *256*, 2741−2759.

(23) Zhao, Y.; Zhu, J.; He, W.; Yang, Z.; Zhu, Y.; Li, Y.; Zhang, J.; Guo, Z. Oxidative DNA Cleavage Promoted by Multinuclear Copper Complexes: Activity Dependence on the Complex Structure. *Chem. - Eur. J.* **2006**, *12*, 6621−6629.

(24) (a) Chufán, E. E.; Puiu, S. C.; Karlin, K. D. Heme-Copper/Dioxygen Adduct Formation, Properties, and Reactivity. *Acc. Chem. Res.* **2007**, *40*, 563−572. (b) Solomon, E. I.; Sarangi, R.; Woertink, J. S.; Augustine, A. J.; Yoon, J.; Ghosh, S. O_2 and N_2O Activation by Bi-, Tri-, and Tetranuclear Cu Clusters in Biology. *Acc. Chem. Res.* **2007**, *40*, 581−591.

(25) Tegoni, M.; Remelli, M. Metallacrowns of Copper(II) and Aminohydroxamates: Thermodynamics of Self-Assembly and Host-Guest Equilibria. *Coord. Chem. Rev.* **2012**, *256*, 289−315.

(26) Zhang, Z. H.; Song, Y.; Okamura, T.; Hasegawa, Y.; Sun, W. Y.; Ueyama, N. Syntheses, Structures, Near-Infrared and Visible Luminescence, and Magnetic Properties of Lanthanide-Organic

Frameworks with an Imidazole-Containing Flexible Ligand. *Inorg. Chem.* **2006**, *45*, 2896−2902.
(27) (a) Curtiss, A. B. S.; Bera, M.; Musie, G. T.; Powell, D. R. Synthesis and Characterization of Mono- and μ_6-sulfato Hexanuclear Zinc Complexes of A New Symmetric Dinucleating Ligand. *Dalton Trans.* **2008**, 2717. (b) Haldar, S.; Dutta, N.; Vijaykumar, V.; Das, A.; Carrella, L.; Oliver, A.; Bera, M. Synthesis, Structure and Properties of New Heterometallic Octanuclear $Li_2Na_2Cu_4$ and Decanuclear Li_2Zn_8 Complexes. *Polyhedron* **2019**, *172*, 58−66.
(28) Redshaw, C.; Elsegood, M. R. J.; Frese, J. W. A.; Ashby, S.; Chao, Y.; Mueller, A. Cellular Uptake Studies of Two Hexanuclear, Carboxylate Bridged, Zinc Ring Structures Using Fluorescence Microscopy. *Chem. Commun.* **2012**, *48*, 6627−6629.
(29) Gennarini, F.; David, R.; López, I.; Mest, Y. L.; Reglier, M.; Belle, C.; Thibon-Pourret, A.; Jamet, H.; Poul, N. L. Influence of Asymmetry on the Redox Properties of Phenoxo- and Hydroxo-Bridged Dicopper Complexes: Spectroelectrochemical and Theoretical Studies. *Inorg. Chem.* **2017**, *56*, 7707−7719.
(30) (a) Patterson, M. R.; Rasika Dias, H. V. Tetranuclear and Trinuclear Copper(I) Pyrazolates as Catalysts in Copper Mediated Azide-Alkyne Cycloadditions (CuAAC). *Dalton Trans.* **2021**, *51*, 375−383. (b) Busch, J. M.; Koshelev, D. S.; Vashchenko, A. A.; Fuhr, O.; Nieger, M.; Utochnikova, V. V.; Brase, S. Various Structural Design Modifications: *para*-Substituted Diphenylphosphinopyridine Bridged Cu(I) Complexes in Organic Light-Emitting Diodes. *Inorg. Chem.* **2021**, *60*, 2315−2332.
(31) Nakajima, T.; Kamiryo, Y.; Hachiken, K.; Nakamae, K.; Ura, Y.; Tanase, T. Tri- and Tetranuclear Copper Hydride Complexes Supported by Tetradentate Phosphine Ligands. *Inorg. Chem.* **2018**, *57*, 11005−11018.
(32) Dutta, N.; Haldar, S.; Majumder, A.; Vijaykumar, G.; Carrella, L.; Bera, M. Synthesis, Structure and Properties of A Novel Self-Assembled Tetranuclear Copper(II) Complex Derived from Carboxylate-Based Multidentate Ligand. *Inorg. Chem. Commun.* **2020**, *121*, 108208.
(33) Majumder, A.; Dutta, N.; Dey, S.; Sow, P.; Samadder, A.; Vijaykumar, G.; Rangan, K.; Bera, M. A Family of $[Zn_6]$ Complexes from the Carboxylate-Bridge-Supported Assembly of $[Zn_2]$ Building Units: Synthetic, Structural, Spectroscopic, and Systematic Biological Studies. *Inorg. Chem.* **2021**, *60*, 17608−17626.
(34) Dutta, N.; Haldar, S.; Vijaykumar, G.; Paul, S.; Chattopadhyay, A. P.; Carrella, L.; Bera, M. Phosphatase-like Activity of Tetranuclear Iron(III) and Zinc(II) Complexes. *Inorg. Chem.* **2018**, *57*, 10802−10820.
(35) Redshaw, C.; Elsegood, M. R. J. Synthesis of Tetra-, Hexa-, and Octanuclear Organozinc Ring Systems. *Angew. Chem., Int. Ed.* **2007**, *46*, 7453−7457.
(36) Grala, A.; Wolska-Pietkiewicz, M.; Wojewódzka, A.; Dabergut, M.; Justyniak, I.; Lewiński, J. Structural Diversity of Ethylzinc Carboxylates. *Organometallics* **2015**, *34*, 4959−4964.
(37) Carlsson, H.; Haukka, M.; Bousseksou, A.; Latour, J. M.; Nordlander, E. Nickel Complexes of Carboxylate-Containing Polydentate Ligands as Models for the Active Site of Urease. *Inorg. Chem.* **2004**, *43*, 8252−8262.
(38) Bera, M.; Musie, G. T.; Powell, D. R. Synthesis and Characterization of New Mono- and Heptazinc Complexes with Unusual Amide Coordination Modes. *Inorg. Chem.* **2009**, *48*, 4625−4627.
(39) Patra, A.; Sen, T. K.; Ghorai, A.; Musie, G. T.; Mandal, S. K.; Ghosh, U.; Bera, M. Synthesis, Structure, Spectroscopic Characterization, and Protein Binding Affinity of New Water-Soluble Hetero- and Homometallic Tetranuclear $[Cu^{II}_2Zn^{II}_2]$ and $[Cu^{II}_4]$ Clusters. *Inorg. Chem.* **2013**, *52*, 2880−2890.
(40) Stewart, C. D.; Arman, H.; Bawazir, H.; Musie, G. T. Synthesis, Characterization, and Spectroscopic Investigation of New Iron(III) and Copper(II) Complexes of a Carboxylate Rich Ligand and Their Interaction with Carbohydrates in Aqueous Solution. *Inorg. Chem.* **2014**, *53*, 10974−10988.
(41) (a) Wannarit, N.; Siriwong, K.; Chaichit, N.; Youngme, S.; Costa, R.; Moreira, I. de P. R.; Illas, F. New Series of Triply Bridged Dinuclear Cu(II) Compounds: Synthesis, Crystal Structure, Magnetic Properties, and Theoretical Study. *Inorg. Chem.* **2011**, *50*, 10648−10659. (b) Costa, R.; Moreira, I. de P. R.; Youngme, S.; Siriwong, K.; Wannarit, N.; Illas, F. Toward the Design of Ferromagnetic Molecular Complexes: Magnetostructural Correlations in Ferromagnetic Triply Bridged Dinuclear Cu(II) Compounds Containing Carboxylato and Hydroxo Bridges. *Inorg. Chem.* **2010**, *49*, 285−294.
(42) (a) Julve, M.; Gleizes, A.; Chamoreau, L. M.; Ruiz, E.; Verdaguer, M. Antiferromagnetic Interactions in Copper(II) μ-Oxalato Dinuclear Complexes: The Role of the Counterion. *Eur. J. Inorg. Chem.* **2018**, *2018*, 509−516. (b) Mukherjee, D.; Nag, P.; Shteinman, A. A.; Vennapusa, S. R.; Mandal, U.; Mitra, M. Catechol Oxidation Promoted by Bridging Phenoxo Moieties in a Bis(μ-phenoxo)-Bridged Dicopper(II) Complex. *RSC Adv.* **2021**, *11*, 22951−22959. (c) Mendoza-Quijano, M. R.; Ferrer-Sueta, G.; Flores-Álamo, M.; Aliaga-Alcalde, N.; Gómez-Vidales, V.; Ugalde-Saldívara, V. M.; Gasque, L. Mechanistic Insight on the Catecholase Activity of Dinuclear Copper Complexes with Distant Metal Centers. *Dalton Trans.* **2012**, *41*, 4985−4997.
(43) (a) Kintzel, B.; Bohme, M.; Liu, J.; Burkhardt, A.; Mrozek, J.; Buchholz, A.; Ardavan, A.; Plass, W. Molecular Electronic Spin Qubits from A Spin-Frustrated Trinuclear Copper Complex. *Chem. Commun.* **2018**, *54*, 12934−12937. (b) Seppälä, P.; Colacio, E.; Mota, A. J.; Sillanpää, R. Synthesis, Crystal Structures and Magnetic Properties of Bis(μ-dialkoxo)-Bridged Linear Trinuclear Copper(II) Complexes with Aminoalcohol Ligands: A Theoretical/Experimental Magneto-Structural Study. *Dalton Trans.* **2012**, *41*, 2648−2658.
(44) (a) Ahmed, N.; Tripathi, S.; Sarkar, A.; Ansari, K. U.; Das, C.; Prajesh, N.; Horike, S.; Boomishankarb, R.; Shanmugam, M. Chiral Tetranuclear Copper(II) Complexes: Syntheses, Optical and Magnetic Properties. *New J. Chem.* **2020**, *44*, 16845−16855. (b) Seppälä, P.; Colacio, E.; Mota, A. J.; Sillanpää, R. Structural Diversity due to Amino Alcohol Ligands Leading to Rare μ_4-Hydroxo-Bridged Tetranuclear and "Bicapped Cubane" Cores in Copper(II) Complexes: A Theoretical and Experimental Magnetostructural Study. *Inorg. Chem.* **2013**, *52*, 11096−11109.
(45) Patra, A.; Haldar, S.; Vijaykumar, G.; Carrella, L.; Ghosh, A. K.; Bera, M. New Symmetrical Dinucleating Ligand Based Assembly of Bridged Dicopper(II) and Dizinc(II) Centers: Synthesis, Structure, Spectroscopy, Magnetic Properties and Glycoside Hydrolysis. *Inorg. Chim. Acta* **2015**, *436*, 195−204.
(46) Majumder, A.; Dutta, N.; Haldar, S.; Das, A.; Carrella, L.; Bera, M. Aromatic Dicarboxylate Incorporated New Di- and Tetranuclear Cobalt(II) Complexes: Synthetic and Structural Aspects, and Evaluation of Properties and Catalytic Activity. *Inorg. Chim. Acta* **2020**, *510*, 119752.
(47) Majumder, A.; Dutta, N.; Das, A.; Carrella, L.; Bera, M. Exploring New Water Soluble Bridged Dicopper(II) Assemblies: Synthesis, Structure, Spectroscopic Characterization, Properties, and Their Interactions with D-glucosamine. *Polyhedron* **2021**, *208*, 115417.
(48) Haldar, S.; Vijaykumar, G.; Carrella, L.; Musie, G. T.; Bera, M. Structure and Properties of A Novel Staircase-Like Decanuclear $[Cu^{II}_{10}]$ Cluster Supported by Carbonate and Carboxylate Bridges. *New J. Chem.* **2018**, *42*, 1276−1283.
(49) Geary, W. J. The Use of Conductivity Measurements in Organic Solvents for the Characterisation of Coordination Compounds. *Coord. Chem. Rev.* **1971**, *7*, 81−122.
(50) Giri, G. C.; Patra, A.; Vijaykumar, G.; Carrella, L.; Bera, M. Hydrolytically Active Tetranuclear $[Ni^{II}_2]_2$ Complexes: Synthesis, Structure, Spectroscopy and Phosphoester Hydrolysis. *RSC Adv.* **2015**, *5*, 99270−99283.
(51) Deacon, G. B.; Phillips, R. J. Relationships Between the Carbon Oxygen Stretching Frequencies of Carboxylato Complexes and the Type of Carboxylate Coordination. *Coord. Chem. Rev.* **1980**, *33*, 227−250.

https://doi.org/10.1021/acsomega.2c04627
ACS Omega 2022, 7, 39985−39997

(52) Zelenak, V.; Vargova, Z.; Gyoryova, K. Correlation of Infrared Spectra of Zinc(II) Carboxylates with Their Structures. *Spectrochim. Acta, Part A* **2007**, *66*, 262−272.
(53) Arora, H.; Lloret, F.; Mukherjee, R. Molecular Squares of Ni^{II} and Cu^{II}: Ferromagnetic Exchange Interaction Mediated by *syn-anti* Carboxylate-Bridging. *Dalton Trans.* **2009**, 9759−9769.
(54) Cotton, F. A.; Wilkinson, G. *Inorganic Chemistry*, 5th ed.; Wiley: 1988; pp 765−775.
(55) Massoud, S. S.; Spell, M.; Ledet, C. C.; Junk, T.; Herchel, R.; Fischer, R. C.; Trávníček, Z.; Mautner, F. A. Magnetic and Structural Properties of Dinuclear Singly Bridged-Phenoxido Metal(II) Complexes. *Dalton Trans.* **2015**, *44*, 2110−2121.
(56) Sheoran, M.; Bhar, K.; Jain, S.; Rana, M.; Khan, T. A.; Sharma, A. K. Phenoxo-Bridged Dicopper Complexes: Syntheses, Characterizations, Crystal Structures and Catecholase Activity. *Polyhedron* **2019**, *161*, 169−178.
(57) West, A. R. *Solid State Chemistry and Its Applications*; Wiley: 1984; pp 553−560.
(58) Bain, G. A.; Berry, J. F. Diamagnetic Corrections and Pascal's Constants. *J. Chem. Educ.* **2008**, *85*, 532−536.
(59) (a) Mukherjee, A.; Rudra, I.; Nethaji, M.; Ramasesha, S.; Chakravarty, A. R. Synthesis, Crystal Structure, and Magnetic Properties of an Alkoxo-Hydroxo-Bridged Octanuclear Copper(II) Complex Showing Chemically Significant Hydrogen-Bonding Interactions Involving a Metallamacrocyclic Core. *Inorg. Chem.* **2003**, *42*, 463−468. (b) Manna, S. C.; Paul, A.; Zangrando, E.; Figuerola, A. Structure and Magnetic Characterization of Tetranuclear Closed/Double-Open Cubane Core, and 1D Polynuclear Copper(II) Complexes. *J. Solid State Chem.* **2019**, *271*, 378−385.
(60) Dias, S. S. P.; Andre, V.; Klak, J.; Duarte, M. T.; Kirillov, A. M. Topological Diversity of Supramolecular Networks Constructed from Copper(II) Aminoalcohol Blocks and 2,6-Naphthalenedicarboxylate Linkers: Self-Assembly Synthesis, Structural Features, and Magnetic Properties. *Cryst. Growth Des.* **2014**, *14*, 3398−3407.
(61) Putz, H.; Brandenburg, K. *Diamond - Crystal and Molecular Structure Visualization (DIAMOND; Ver. 4.0)*; 2014.
(62) Addison, A.; Rao, T. N.; Reedijk, J.; van Rijn, J.; Verschoor, G. C. Synthesis, Structure, and Spectroscopic Properties of Copper(II) Compounds Containing Nitrogen-Sulphur Donor Ligands; The Crystal and Molecular Structure of Aqua[1,7- bis(*N* -methylbenzimidazol-2′-yl)-2,6-dithiaheptane] Copper(II) Perchlorate. *J. Chem. Soc., Dalton Trans.* **1984**, 1349−1356.
(63) Bhunia, A.; Mistri, S.; Manne, R. K.; Santra, M. K.; Manna, S. C. Synthesis, Crystal Structure, Cytotoxicity Study, DNA/Protein Binding and Molecular Docking of Dinuclear Copper(II) Complexes. *Inorg. Chim. Acta* **2019**, *491*, 25−33.
(64) Seppala, P.; Colacio, E.; Mota, A. J.; Sillanpaa, R. Dinuclear Alkoxo-Bridged Copper(II) Coordination Polymers: Syntheses, Structural and Magnetic Properties. *Inorg. Chim. Acta* **2010**, *363*, 755−762.
(65) Weng, C. H.; Cheng, S. C.; Wei, H. M.; Wei, H. H.; Lee, C. J. Magnetostructural Correlations and Catecholase-Like Activities of μ-Alkoxo-μ-Carboxylato Double Bridged Dinuclear and Tetranuclear Copper(II) Complexes. *Inorg. Chim. Acta* **2006**, *359*, 2029−2040.
(66) Joy, R. A.; Arman, H.; Xiang, S.; Musie, G. T. *Inorg. Chim. Acta* **2013**, *394*, 220−228.
(67) (a) Esteves, C. V.; Mateus, P.; Andre, V.; Bandeira, N. A. G.; Calhorda, M. J.; Ferreira, L. P.; Delgado, R. Di- versus Trinuclear Copper(II) Cryptate for the Uptake of Dicarboxylate Anions. *Inorg. Chem.* **2016**, *55*, 7051−7060.
(68) Löffler, M.; Gregoliński, J.; Korabik, M.; Lis, T.; Lisowski, J. Multinuclear Ni(II), Cu(II) and Zn(II) Complexes of Chiral Macrocyclic Nonaazamine. *Dalton Trans.* **2016**, *45*, 15586−15594.
(69) Salvadeo, E.; Dubois, L.; Latour, J. Trinuclear Copper Complexes as Biological Mimics: Ligand Designs and Reactivities. *Coord. Chem. Rev.* **2018**, *374*, 345−375.
(70) (a) Liu, X.; Liu, H.; Cen, P.; Chen, X.; Zhou, H.; Song, W.; Hu, Q. Auxiliary Ligand-Triggered Assembly of Two Dinuclear Cu(II) Compounds with a Pyridylhydrazone Derivative: Synthesis, Crystal Structure and Magnetic Property. *Inorg. Chim. Acta* **2016**, *447*, 12−17. (b) Cotton, F. A.; Lewis, G. E.; Mott, G. N. Dinuclear and Polynuclear Oxovanadium(IV) Compounds: A Complicated Sodium Oxovanadium(IV) Trifluoroacetate Compound, $Na_4(VO)_2(CF_3CO_2)_8(THF)_6(H_2O)_2$. *Inorg. Chem.* **1983**, *22*, 1825−1827. (c) Clegg, W.; Little, I. R.; Straughan, B. P. Zinc Carboxylate Complexes: Structural Characterization of the Mixed-Metal Linear Trinuclear Complexes $MZn_2(crot)_6(base)_2$ (M = Mn, Co, Ni, Zn, Cd, Mg, Ca, Sr; crot- = crotonate(1-); base = quinoline, 6-methylquinoline). *Inorg. Chem.* **1988**, *27*, 1916−1923.
(71) (a) Gu, Y. N.; Zhao, D.; Yu, H.; Ge, R.; Li, Z.; Tian, C. B.; Li, X. X.; Sun, Y. Q.; Zheng, S. T. Incorporating Polyoxometalates and Organic Ligands to Pursue 3d-4f Heterometallic Clusters: A Series of $\{Cr_4Ln_4\}$ Clusters Stabilized by Phthalic Acid and $[SiW_{12}O_{40}]^{4-}$. *RSC Adv.* **2019**, *9*, 13543−13549. (b) Hale, A. R.; King, P.; Abboud, K. A.; Christou, G. Unusual Mn_5 Cluster with A 'Twisted Bow-Tie' Topology and $Mn^{II}Mn^{III}{}_2$ $Mn^{IV}{}_2$ Oxidation States: Synthesis, Structure, and Magnetic Properties. *Polyhedron* **2021**, *200*, 115141.
(72) Haldar, S.; Vijaykumar, G.; Carrella, L.; Batha, S.; Musie, G. T.; Bera, M. Inorganic Phosphate and Arsenate within New Tetranuclear Copper and Zinc Complexes: Syntheses, Crystal Structures, Magnetic, Electrochemical, and Thermal Studies. *ACS Omega* **2017**, *2*, 1535−1549.
(73) Chen, T.; Li, M.; Liu, J. $\pi-\pi$ Stacking Interaction: A Nondestructive and Facile Means in Material Engineering for Bioapplications. *Cryst. Growth Des.* **2018**, *18*, 2765−2783.
(74) Hunter, C. A.; Sanders, J. K. M. The Nature of pi-pi Interactions. *J. Am. Chem. Soc.* **1990**, *112*, 5525−5534.
(75) Shaban, S. Y.; Ramadan, A. E. M.; Ibrahim, M. M.; Mohamed, M. A.; van Eldik, R. Spectroscopic, Thermodynamic, Kinetic Studies and Oxidase/Antioxidant Biomimetic Catalytic Activities of Tris(3,5-Dimethylpyrazolyl)Borate Cu(II) Complexes. *Dalton Trans.* **2015**, *44*, 14110−14121.
(76) Rocha, M.; Ruiz, M. C.; Echeverri, G. A.; Piro, O. E.; Virgilio, A. L. D.; Leon, I. E.; Frontera, A.; Gil, D. M. Diethylaminophenyl-Based Schiff Base Cu(II) and V(IV) Complexes: Experimental and Theoretical Studies and Cytotoxicity Assays. *New J. Chem.* **2019**, *43*, 18832−18842.
(77) Paquet, C.; Lacelle, T.; Liu, X.; Deore, B.; Kell, A. J.; Lafrenière, S.; Malenfant, P. R. L. The Role of Amine Ligands in Governing Film Morphology and Electrical Properties of Copper Films Derived From Copper Formate-Based Molecular Inks. *Nanoscale* **2018**, *10*, 6911−6921.
(78) Fouad, R.; Shaaban, I. A.; Ali, T. E.; Assiri, M. A.; Shenouda, S. S. Co(II), Ni(II), Cu(II) and Cd(II)-Thiocarbonohydrazone Complexes: Spectroscopic, DFT, Thermal, and Electrical Conductivity Studies. *RSC Adv.* **2021**, *11*, 37726−37743.
(79) Zhu, D.; Zheng, F.; Xu, S.; Zhang, Y.; Chen, Q. MOF-Derived Self-Assembled ZnO/Co_3O_4 Nanocomposite Clusters as High-Performance Anodes for Lithium-Ion Batteries. *Dalton Trans* **2015**, *44*, 16946−16952.
(80) *APEX-II, SAINT-Plus, and TWINABS*; Bruker-Nonius AXS Inc.: 2004.
(81) Sheldrick, G. M. *SADABS. Program for Multi-Scan Absorption Correction of Area Detector Data*; University of Göttingen: 2002.
(82) Altomare, A.; Burla, M. C.; Camalli, M.; Cascarano, G. L.; Giacovazzo, C.; Guagliardi, A.; Moliterni, A. G. G.; Polidori, G.; Spagna, R. *SIR97*: A New Tool for Crystal Structure Determination and Refinement. *J. Appl. Crystallogr.* **1999**, *32*, 115−119.
(83) (a) Sheldrick, G. M. Crystal Structure Refinement with *SHELXL*. *Acta Crystallogr.* **2015**, *C71*, 3−8. (b) *International Tables for Crystallography*; Kluwer: Boston, 1995; Vol. *C*, Tables 6.1.1.4, 4.2.6.8, and 4.2.4.2.
(84) Dolomanov, O. V.; Bourhis, L. J.; Gildea, R. J.; Howard, J. A. K.; Puschmann, H. *OLEX2*: A Complete Structure Solution, Refinement and Analysis Program. *J. Appl. Crystallogr.* **2009**, *42*, 339−341.

https://doi.org/10.1021/acsomega.2c04627
ACS Omega 2022, 7, 39985−39997